Nuclear physics aspects of double beta decay

Petr Vogel

Kellogg Radiation Laboratory 106-38
California Institute of Technology
Pasadena, CA 91125, USA

Lecture notes for course CLXX "MEASUREMENTS OF NEUTRINO MASS"
Int. School of Physics "Enrico Fermi", Varenna, June 2008

Summary. —
Comprehensive description of the phenomenology of the $\beta\beta$ decay is given, with emphasis on the nuclear physics aspects. After a brief review of the neutrino oscillation results and of motivation to test the lepton number conservation, the mechanism of the $0\nu\beta\beta$ is discussed. Its relation to the lepton flavor violation involving charged leptons and its use as a diagnostic tool of the $0\nu\beta\beta$ mechanism is described. Next the basic nuclear physics of both $\beta\beta$-decay modes is presented, and the decay rate formulae derived. The nuclear physics methods used, the nuclear shell model and the quasiparticle random phase approximation, are described next, and the choice of input parameters is discussed in the following section. Finally, the numerical values of the nuclear matrix elements, and their uncertainty, are presented. In the appendix the relation of the search for the neutrino magnetic moment to the Dirac versus Majorana nature of neutrinos is described.

PACS 21.60.-n – .
PACS 23.40.Bw – .
PACS 23.40.Hc – .

1. – Introduction to $\beta\beta$ decay

In the last decade neutrino oscillation experiments have convincingly and triumphantly shown that neutrinos have a finite mass and that the lepton flavor is not a conserved quantity. These results opened the door to what is often called the "Physics Beyond the Standard Model". In other words, accommodating these findings into a consistent scenario requires generalization of the Standard Model of electroweak interactions that postulates that neutrinos are massless and that consequently lepton flavor, and naturally, also the total lepton number, are conserved quantities.

In oscillation experiments only the differences in squares of the neutrino masses, $\Delta m^2 \equiv |m_2^2 - m_1^2|$, is measured, and the results do not depend on the charge conjugation properties of neutrinos, i.e. whether they are Dirac or Majorana fermions. Nevertheless, from oscillation experiments one can establish a lower limit on the absolute value of the neutrino mass scale, $m_{scale} = \sqrt{|\Delta m^2|}$. Thus, one or more neutrinos have a mass of at least $\sqrt{|\Delta m^2_{atm}|} \sim 50$ meV, and another one has mass of at least $\sqrt{|\Delta m^2_{sol}|} \sim 10$ meV. In addition, an upper limit on the masses of all active neutrinos ~ 2 - 3 eV can be derived from the combination of analysis of the tritium beta-decay experiments and the neutrino oscillation experiments. Combining these constraints, masses of at least two (out of the total of three active) neutrinos are bracketted by 10 meV $\leq m_\nu \leq 2$ - 3 eV.

Thus, neutrino masses are six or more orders of magnitude smaller than the masses of the other fermions. Moreover, the pattern of masses, i.e. the mass ratios of neutrinos, is rather different (even though it remains largely unknown) than the pattern of masses of the up- or down-type quarks or charged leptons. All of these facts suggest that, perhaps, the origin of the neutrino mass is different than the origin (which is still not well understood) of the masses of the other fermions.

The discoveries of neutrino oscillations, in turn, are causing a renaissance of enthusiasm in the double beta decay community and a slew of new experiments that are expected to reach, within a near future, the sensitivity corresponding to the neutrino mass scale. Below I review the current status of the double beta decay and the effort devoted to reach the required sensitivity, as well as various issues in theory (or phenomenology) related to the relation of the $0\nu\beta\beta$ decay rate to the absolute neutrino mass scale and to the general problem of the Lepton Number Violation (LNV). And, naturally, substantial emphasis is devoted to the nuclear structure issues. But before doing that I very briefly summarize the achievements of the neutrino oscillation searches and the role that the search for the neutrinoless double beta decay plays in the elucidation of the pattern of neutrino masses and mixing.

There is a consensus that the measurement of atmospheric neutrinos by the SuperKamiokande collaboration[1] can be only interpreted as a consequence of the nearly maximum mixing between ν_μ and ν_τ neutrinos, with the corresponding mass squared difference $|\Delta m^2_{atm}| \sim 2.4 \times 10^{-3}\text{eV}^2$. This finding was confirmed by the K2K experiment [2] that uses accelerator ν_μ beam pointing towards the SuperKamiokande detector 250 km away as well as by the very recent result of the MINOS experiment located at the Sudan mine in Minnesota 735 km away from Fermilab[3]. Several large long-baseline

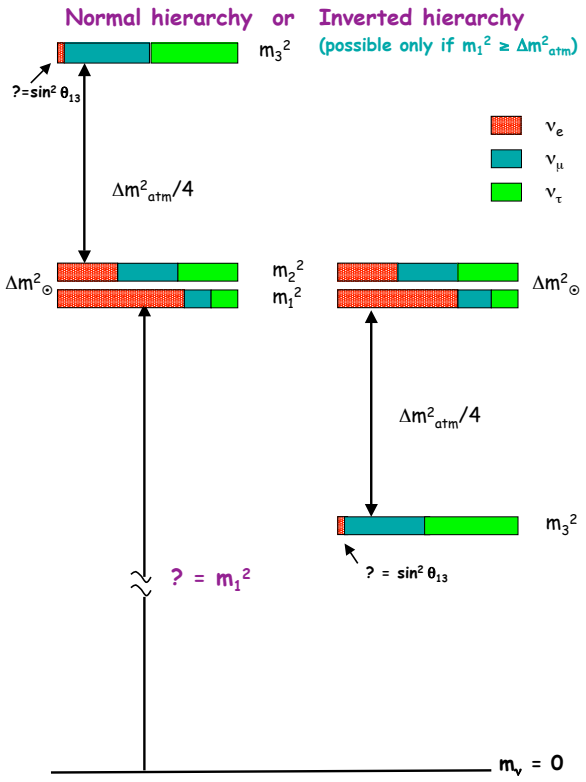

Fig. 1. – Schematic illustration of the decomposition of the neutrino mass eigenstates ν_i in terms of the flavor eigenstates. The two hierarchies cannot be, at this time, distinguished. The small admixture of ν_e into ν_3 is an upper limit, and the mass square of the neutrino ν_1, the quantity m_1^2, remains unknown.

experiments are being build to further elucidate this discovery, and determine the corresponding parameters even more accurately.

At the same time the "solar neutrino puzzle", which has been with us for over thirty years since the pioneering chlorine experiment of Davis[4], also reached the stage where the interpretation of the measurements in terms of oscillations between the ν_e and some combination of active, i.e., ν_μ and ν_τ neutrinos, is inescapable. In particular, the juxtaposition of the results of the SNO experiment[5] and SuperKamiokande[6], together with the earlier solar neutrino flux determination in the gallium experiments[7, 8] and, of course chlorine[4], leads to that conclusion. The value of the corresponding oscillation parameters, however, remained uncertain, with several "solutions" possible, although the so-called Large Mixing Angle (LMA) solution with $\sin^2 2\theta_{sol} \sim 0.8$ and $\Delta m^2_{sol} \sim 10^{-4}\mathrm{eV}^2$

was preferred. A decisive confirmation of the "solar" oscillations was provided by the nuclear reactor experiment KamLAND [9, 10, 11] that demonstrated that the flux of the reactor $\bar{\nu}_e$ is reduced and its spectrum distorted at the distance $L_0 \sim 180$ km from nuclear reactors. The most recent KamLAND results [11], combined with the existing solar neutrino data launched the era of precision neutrino measurements, with the corresponding parameters $\Delta m^2_{21} = 7.59^{+0.21}_{-0.21} \times 10^{-5}\text{eV}^2$ and $\tan^2\theta_{12} = 0.47^{+0.06}_{-0.05}$ determined with an unprecedented accuracy. Analysis of that experiment, moreover, clearly shows the oscillatory behavior of the detection probability as a function of L_0/E_ν. That behavior can be traced in ref. [11] over two full periods.

The pattern of neutrino mixing is further simplified by the constraint due to the Chooz and Palo Verde reactor neutrino experiments[12, 13] which lead to the conclusion that the third mixing angle, θ_{13}, is small, $\sin^2 2\theta_{13} \leq 0.1$. The two remaining possible neutrino mass patterns are illustrated in Fig.1.

As already stated, oscillation experiments cannot determine the absolute magnitude of the masses and, in particular, cannot at this stage separate two rather different scenarios, the hierarchical pattern of neutrino masses in which $m \sim \sqrt{\Delta m^2}$ and the degenerate pattern in which $m \gg \sqrt{\Delta m^2}$. It is hoped that the search for the neutrinoless double beta decay, reviewed here, will help in foreseeable future in determining or at least narrowing down the absolute neutrino mass scale, and in deciding which of these two possibilities is applicable.

Moreover, even more important is the fact that the oscillation results do not tell us anything about the properties of neutrinos under charge conjugation. While the charged leptons are Dirac particles, distinct from their antiparticles, neutrinos may be the ultimate neutral particles, as envisioned by Majorana, that are identical to their antiparticles. That fundamental distinction becomes important only for massive particles. Neutrinoless double beta decay proceeds only when neutrinos are massive Majorana particles, hence its observation would resolve the question.

The argument for the "Majorana nature" of the neutrinos can be traced to the observation by Weinberg [14] who pointed out almost thirty year ago that there exists only one lowest order (dimension 5, suppressed by only one inverse power of the corresponding high energy scale Λ) gauge-invariant operator given the content of the standard model

$$\mathcal{L}^{(5)} = C^{(5)}/\Lambda(\bar{L}^c \epsilon H)(H^T \epsilon L) \ , \tag{1}$$

where L is the lepton doublet, $\bar{L}^c = L^T C$ with C the charge conjugation operator, $\epsilon = -i\tau_2$, and H represent the Higgs boson. After the spontaneous symmetry breaking the Higgs acquires vacuum expectation value and the above operator represents the neutrino Majorana mass that violates the total lepton number conservation law by two units

$$\mathcal{L}^{(M)} = \frac{C^{(5)}}{\Lambda}\frac{v^2}{2}(\bar{\nu}^c \nu) + h.c. \ , \tag{2}$$

where $v \sim 250$ GeV and the neutrinos are naturally light because their mass is suppressed

by the large value of the new physics scale Λ in the denominator.

The most popular explanation of the smallness of neutrino mass is the see-saw mechanism, which is also roughly thirty years old [15]. In it, the existence of heavy right-handed neutrinos N_R is postulated, and by diagonalizing the corresponding mass matrix one arrives at the formula

$$m_\nu = \frac{m_D^2}{M_N} \tag{3}$$

where the Dirac mass m_D is expected to be a typical charged fermion mass and M_N is the Majorana mass of the heavy neutrinos N_R. Again, the small mass of the standard neutrino is related to the large mass of the heavy right-handed partner. Requiring that m_ν is of the order of 0.1 eV means that M_N (or Λ) is $\sim 10^{14-15}$ GeV, i.e. near the GUT scale. That makes this template scenario particularly attractive.

Clearly, one cannot reach such high energy scale experimentally. But, these scenarios imply that neutrinos are Majorana particles, and consequently that the total lepton number should not be conserved. Hence the tests of the lepton number conservation acquires a fundamental importance.

Double beta decay ($\beta\beta$) is a nuclear transition $(Z, A) \rightarrow (Z + 2, A)$ in which two neutrons bound in a nucleus are simultaneously transformed into two protons plus two electrons (and possibly other light neutral particles). This transition is possible and potentially observable because nuclei with even Z and N are more bound than the odd-odd nuclei with the same $A = N + Z$. Analogous transition of two protons into two neutrons are also, in principle, possible in several nuclei, but phase space considerations give preference to the former mode.

An example is shown in Fig. 2. The situation shown there is not really exceptional. There are eleven analogous cases (candidate nuclei) with the Q-value (i.e. the kinetic energy available to leptons) in excess of 2 MeV.

There are two basic modes of the $\beta\beta$ decay. In the two-neutrino mode ($2\nu\beta\beta$) there are 2 $\bar{\nu}_e$ emitted together with the 2 e^-. It is just an ordinary beta decay of two bound neutrons occurring simultaneously since the sequential decays are forbidden by the energy conservation law. For this mode, clearly, the lepton number is conserved and this mode of decay is allowed in the standard model of electroweak interaction. It has been repeatedly observed in a number of cases and proceeds with a typical half-life of $\sim 10^{19-20}$years for the nuclei with Q-values above 2 MeV. In contrast, in the neutrinoless mode ($0\nu\beta\beta$) only the $2e^-$ are emitted and nothing else. That mode clearly violates the law of lepton number conservation and is forbidded in the standard model. Hence, its observation would be a signal of a "new physics".

The two modes of the $\beta\beta$ decay have some common and some distinct features. The common features are:

- The leptons carry essentially all available energy. The nuclear recoil is negligible, $Q/Am_p \ll 1$.

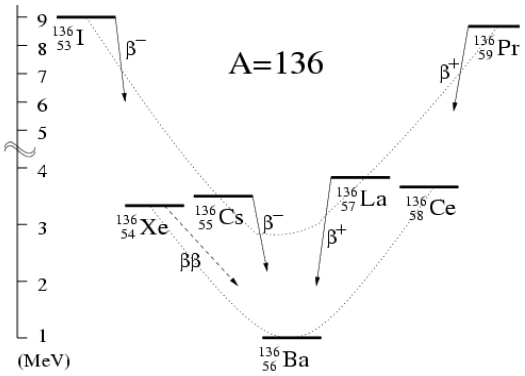

Fig. 2. – Atomic masses of the isotopes with $A = 136$. Nuclei ^{136}Xe, ^{136}Ba and ^{136}Ce are stable against the ordinary β decay; hence they exist in nature. However, energy conservation alone allows the transition $^{136}\text{Xe} \to {}^{136}\text{Ba} + 2e^-$ (+ possibly other neutral light particles) and the analogous decay of ^{136}Ce with the positron emission.

- The transition involves the 0^+ ground state of the initial nucleus and (in almost all cases) the 0^+ ground state of the final nucleus. In few cases the transition to an excited 0^+ or 2^+ state in the final nucleus is energetically possible, but suppressed by the smaller phase space available. (But the $2\nu\beta\beta$ decay to the excited 0^+ state has been observed in few cases.)

- Both processes are of second order of weak interactions, $\sim G_F^4$, hence inherently slow. The phase space consideration alone (for the $2\nu\beta\beta$ mode $\sim Q^{11}$ and for the $0\nu\beta\beta$ mode $\sim Q^5$) give preference to the $0\nu\beta\beta$ which is, however, forbidden by the lepton number conservation.

The distinct features are:

- In the $2\nu\beta\beta$ mode the two neutrons undergoing the transition are uncorrelated (but decay simultaneously) while in the $0\nu\beta\beta$ the two neutrons are correlated.

- In the $2\nu\beta\beta$ mode the sum electron kinetic energy $T_1 + T_2$ spectrum is continuous and peaked below $Q/2$. This is due to the electron masses and the Coulomb attraction. As $T_1 + T_2 \to Q$ the spectrum approaches zero approximately like $(\Delta E/Q)^6$.

- On the other hand in the $0\nu\beta\beta$ mode the sum of the electron kinetic energies is fixed, $T_1 + T_2 = Q$, smeared only by the detector resolution.

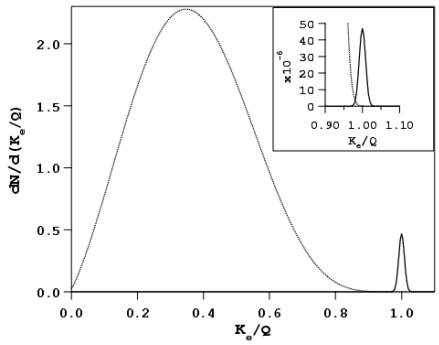

Fig. 3. – Separating the $0\nu\beta\beta$ mode from the $2\nu\beta\beta$ by the shape of the sum electron spectrum, including the effect of the 2% resolution smearing. The figure is for the rate ratio 1/100 and the insert for $1/10^6$.

These last distinct features allow one to separate the two modes experimentally by measuring the sum energy of the emitted electrons with a good energy resolution, even if the decay rate for the $0\nu\beta\beta$ mode is much smaller than for the $2\nu\beta\beta$ mode. This is illustrated in Fig.3 where the insert shows the situation for the rate ratio of $1 : 10^6$ corresponding to the most sensitive current experiments.

Various aspects, both theoretical and experimental, of the $\beta\beta$ decay have been reviewed many times. Here I quote just some of the review articles[16, 17, 18, 19, 20, 21], earlier references can be found there.

In this introductory section let me make only few general remarks. The existence of the $0\nu\beta\beta$ decay would mean that on the elementary particle level a six fermion lepton number violating amplitude transforming two d quarks into two u quarks and two electrons is nonvanishing. As was first pointed out by Schechter and Valle[22] more than twenty years ago, this fact alone would guarantee that neutrinos are massive Majorana fermions (see Fig. 4). This qualitative statement (or theorem), however, does not in general allow us to deduce the magnitude of the neutrino mass once the rate of the $0\nu\beta\beta$ decay have been determined. It is important to stress, however, that quite generally an observation of **any** total lepton number violating process, not only of the $0\nu\beta\beta$ decay, would necessarily imply that neutrinos are massive Majorana fermions.

There is no indication at the present time that neutrinos have nonstandard interactions, i.e. they seem to have only interactions carried by the W and Z bosons that are contained in the Standard Electroweak Model. All observed oscillation phenomena can be understood if one assumes that neutrinos interact exactly the way the Standard Model prescribes, but are massive fermions forcing a generalization of the model. If we accept this, but in addition assume that neutrinos are Majorana particles, we can in fact relate the $0\nu\beta\beta$ decay rate to a quantity containing information about the absolute neutrino

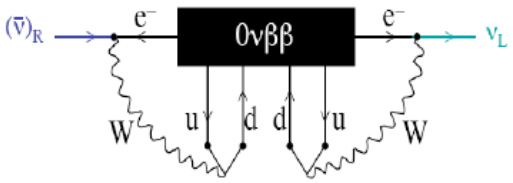

Fig. 4. – By adding loops involving only standard weak interaction processes the $\beta\beta$ decay amplitude (the black box) implies the existence of the Majorana neutrino mass.

mass. With these caveats that relation can be expressed as

$$\frac{1}{T^{0\nu}_{1/2}} = G^{0\nu}(Q,Z)|M^{0\nu}|^2\langle m_{\beta\beta}\rangle^2 \ , \tag{4}$$

where $G^{0\nu}(Q,Z)$ is a phase space factor that depends on the transition Q value and through the Coulomb effect on the emitted electrons on the nuclear charge and that can be easily and accurately calculated (a complete list of the phase space factors $G^{0\nu}(Q,Z)$ and $G^{2\nu}(Q,Z)$ can be found, e.g. in Ref. [23]), $M^{0\nu}$ is the nuclear matrix element that can be evaluated in principle, although with a considerable uncertainty and is discussed in detail later, and finally the quantity $\langle m_{\beta\beta}\rangle$ is the effective neutrino Majorana mass, representing the important particle physics ingredient of the process.

In turn, the effective mass $\langle m_{\beta\beta}\rangle$ is related to the mixing angles θ_{ij} (or to the matrix elements $|U_{e,i}|$ of the neutrino mixing matrix) that are determined or constrained by the oscillation experiments, to the absolute neutrino masses m_i of the mass eigenstates ν_i and to the totally unknown additional parameters, as fundamental as the mixing angles θ_{ij}, the so-called Majorana phases $\alpha(i)$,

$$\langle m_{\beta\beta}\rangle = |\Sigma_i|U_{ei}|^2 e^{i\alpha(i)} m_i| \ . \tag{5}$$

Here U_{ei} are the matrix elements of the first row of the neutrino mixing matrix.

It is straightforward to use eq.(5) and the known neutrino oscillation results in order to compare $\langle m_{\beta\beta}\rangle$ with other neutrino mass related quantities. This is illustrated in Fig.5. Traditionally such plot is made as in the left panel. However, the lightest neutrino mass m_{min} is not an observable quantity. For that reason the other two panels show the relation of $\langle m_{\beta\beta}\rangle$ to the sum of the neutrino masses M that is constrained and perhaps one day will be determined by the "observational cosmology", and also to $\langle m_\beta\rangle$ that represent the parameter that can be determined or constrained in ordinary β decay,

$$\langle m_\beta\rangle^2 = \Sigma_i|U_{ei}|^2 m_i^2 \ . \tag{6}$$

Several remarks are in order. First, the observation of the $0\nu\beta\beta$ decay and determination of $\langle m_{\beta\beta}\rangle$, even when combined with the knowledge of M and/or $\langle m_\beta\rangle$ does not allow, in general, to distinguish between the normal and inverted mass orderings. This is a consequence of the fact that the Majorana phases are unknown. In regions in Fig. 5 where the two hatched bands overlap it is clear that two solutions with the same $\langle m_{\beta\beta}\rangle$ and the same M (or the same $\langle m_\beta\rangle$) always exist and cannot be distinguished.

On the other hand, obviously, if one can determine that $\langle m_{\beta\beta}\rangle \geq 0.1$ eV we would conclude that the mass pattern is degenerate. And in the so far hypothetical case that one could show that $\langle m_{\beta\beta}\rangle \leq 0.01$ eV, but nonvanishing nevertheless, the normal hierarchy would be established([1]).

It is worthwhile noting that if the inverted mass ordering is realized in nature, (and neutrinos are Majorana particles) the quantity $\langle m_{\beta\beta}\rangle$ is constrained from below by $\sim$0.01 eV. This is within the reach of the next generation of experiments. Also, at least in principle, in the case of the normal hierarchy while all neutrinos could be massive Majorana particles it would be still possible that $\langle m_{\beta\beta}\rangle = 0$. Such a situation, however, requires "fine tuning" or reflects a symmetry of some kind. For example, if $\theta_{13} = 0$ the relation $m_1/m_2 = \tan^2\theta_{12}$ must be realized in order that $\langle m_{\beta\beta}\rangle = 0$. This implies, therefore, a definite relation between the neutrino masses and mixing angles. There is only one value of $m_1 = 4.6$ meV for which this condition is valid.

Let us finally remark that the $0\nu\beta\beta$ decay is not the only LNV process for which important experimental constraints exist. Examples of the other LNV processes with important limits are

$$\begin{aligned} &\mu^- + (Z, A) \to e^+ + (Z-2, A);\ \text{exp. branching ratio} \leq 10^{-12}\ , \\ &K^+ \to \mu^+\mu^+\pi^-;\ \text{exp. branching ratio} \leq 3\times 10^{-9}\ , \\ &\bar{\nu}_e \text{ emission from the Sun};\ \text{exp. branching ratio} \leq 10^{-4}\ . \end{aligned} \tag{7}$$

However, detailed analysis suggests that the study of the $0\nu\beta\beta$ decay is by far the most sensitive test of LNV. In simple terms, this is caused by the amount of tries one can make. A 100 kg $0\nu\beta\beta$ decay source contains $\sim 10^{27}$ nuclei that can be observed for a long time (several years). This can be contrasted with the possibilities of first producing muons or kaons, and then searching for the unusual decay channels. The Fermilab accelerators, for example, produce $\sim 10^{20}$ protons on target per year in their beams and thus correspondingly smaller numbers of muons or kaons.

2. – Mechanism of the $0\nu\beta\beta$ decay

It has been recognized long time ago that the relation between the $0\nu\beta\beta$-decay rate and the effective Majorana mass $\langle m_{\beta\beta}\rangle$ is to some extent problematic. The rather con-

([1]) In that case also the $\langle m_\beta\rangle$ in the right panel would not represent the quatity directly related to the ordinary β decay. There are no ideas, however, how to reach the corresponding sensitivity in ordinary β decay at the present time.

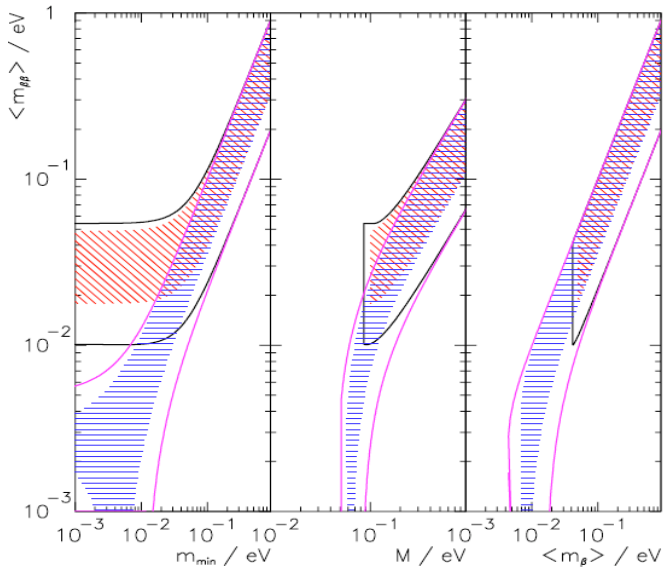

Fig. 5. – The left panel shows the dependence of $\langle m_{\beta\beta}\rangle$ on the absolute mass of the lightest neutrino mass eigenstate m_{min}, the middle one shows the relation between $\langle m_{\beta\beta}\rangle$ and the sum of neutrino masses $M = \Sigma m_i$ determined or costrained by the "observational cosmology", and the right one depicts the relation between $\langle m_{\beta\beta}\rangle$ and the effective mass $\langle m_{\beta}\rangle$ determined or contrained by the ordinary β decay. In all panels the width of the hatched area is due to the unknown Majorana phases and therefore irreducible. The solid lines indicate the allowed regions by taking into account the current uncertainties in the oscillation parameters; they will shrink as the accuracy improves. The two sets of curves correspond to the normal and inverted hierarchies, they merge above about $\langle m_{\beta\beta}\rangle \sim 0.1$ eV, where the degenerate mass pattern begins.

servative assumption leading to eq.(4) is that the only possible way the $0\nu\beta\beta$ decay can occur is through the exchange of a virtual light, but massive, Majorana neutrino between the two nucleons undergoing the transition, and that these neutrinos interact by the standard left-handed weak currents. But that is not the only possible mechanism. LNV interactions involving so far unobserved much heavier ($\sim$ TeV) particles can lead to a comparable $0\nu\beta\beta$ decay rate. Some of the possible mechanisms of the elementary $dd \to uu + e^-e^-$ transition (the "black box in Fig. 4) are indicated in Fig. 6. Only the graph in the upper left corner would lead to eq. (4). Thus, in the absence of additional information about the mechanism responsible for the $0\nu\beta\beta$ decay one could not unambiguously infer the magnitude of $\langle m_{\beta\beta}\rangle$ from the $0\nu\beta\beta$-decay rate.

In general $0\nu\beta\beta$ decay can be generated by (i) light massive Majorana neutrino exchange or (ii) heavy particle exchange (see, e.g. Refs.[24, 25]), resulting from LNV dynamics at some scale Λ above the electroweak one. The relative size of heavy (A_H)

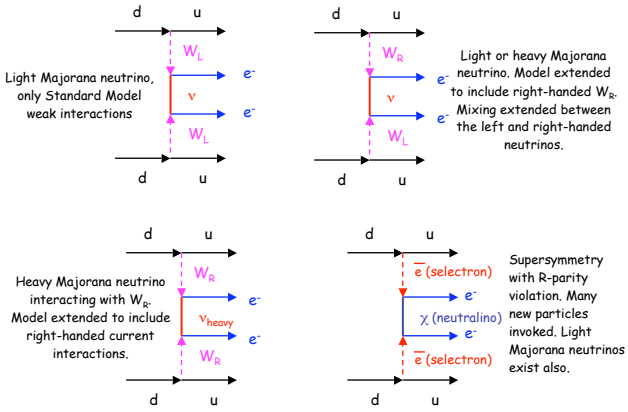

Fig. 6. – All these symbolic Feynman graphs potentially contribute to the $0\nu\beta\beta$-decay amplitude

versus light particle (A_L) exchange contributions to the decay amplitude can be crudely estimated as follows [26]:

$$A_L \sim G_F^2 \frac{\langle m_{\beta\beta}\rangle}{\langle k^2\rangle},\ A_H \sim G_F^2 \frac{M_W^4}{\Lambda^5},\ \frac{A_H}{A_L} \sim \frac{M_W^4\langle k^2\rangle}{\Lambda^5\langle m_{\beta\beta}\rangle}\ , \tag{8}$$

where $\langle m_{\beta\beta}\rangle$ is the effective neutrino Majorana mass, $\langle k^2\rangle \sim (100\ \text{MeV})^2$ is the typical light neutrino virtuality, and Λ is the heavy scale relevant to the LNV dynamics. Therefore, $A_H/A_L \sim O(1)$ for $\langle m_{\beta\beta}\rangle \sim 0.1 - 0.5$ eV and $\Lambda \sim 1$ TeV, and thus the LNV dynamics at the TeV scale leads to similar $0\nu\beta\beta$-decay rate as the exchange of light Majorana neutrinos with the effective mass $\langle m_{\beta\beta}\rangle \sim 0.1 - 0.5$ eV.

Obviously, the lifetime measurement by itself does not provide the means for determining the underlying mechanism. The spin-flip and non-flip exchange can be, in principle, distinguished by the measurement of the single-electron spectra or polarization (see e.g. [27]). However, in most cases the mechanism of light Majorana neutrino exchange, and of heavy particle exchange cannot be separated by the observation of the emitted electrons. Thus one must look for other phenomenological consequences of the different mechanisms. Here I discuss the suggestion[28] that under natural assumptions the presence of low scale LNV interactions, and therefore the absence of proportionality between $\langle m_{\beta\beta}\rangle^2$ and the $0\nu\beta\beta$-decay rate also affects muon lepton flavor violating (LFV) processes, and in particular enhances the $\mu \to e$ conversion compared to the $\mu \to e\gamma$ decay.

The discussion is concerned mainly with the branching ratios $B_{\mu\to e\gamma} = \Gamma(\mu \to e\gamma)/\Gamma_\mu^{(0)}$ and $B_{\mu\to e} = \Gamma_{\rm conv}/\Gamma_{\rm capt}$, where $\mu \to e\gamma$ is normalized to the standard muon decay rate $\Gamma_\mu^{(0)} = (G_F^2 m_\mu^5)/(192\pi^3)$, while $\mu \to e$ conversion is normalized to the capture

rate $\Gamma_{\rm capt}$. The main diagnostic tool in our analysis is the ratio

$$\mathcal{R} = B_{\mu\to e}/B_{\mu\to e\gamma} \ , \tag{9}$$

and the relevance of our observation relies on the potential for LFV discovery in the forthcoming experiments MEG [29] ($\mu \to e\gamma$) and MECO [30] ($\mu \to e$ conversion)([2]).

At present, the most stringent limit on the branching ratio $B_{\mu\to e\gamma}$ is [31] 1.2×10^{-11} and the MEG experiment aims at the sensitivity about two orders of magnitude better. For the muon conversion the best experimental limit [32] used gold nuclei and reached $B_{\mu\to e} < 8 \times 10^{-13}$. The various proposals aim at reaching sensitivity of about 10^{-17}.

It is useful to formulate the problem in terms of effective low energy interactions obtained after integrating out the heavy degrees of freedom that induce LNV and LFV dynamics. Thus, we will be dealing only with the Standard Model particles and all symmetry relations will be obeyed. However, operators of dimension > 4 will be suppressed by $1/\Lambda^{d-4}$, where Λ is the scale of new physics. If the scales for both LNV and LFV are well above the weak scale, then one would not expect to observe any signal in the forthcoming LFV experiments, nor would the effects of heavy particle exchange enter $0\nu\beta\beta$ at an appreciable level. In this case, the only origin of a signal in $0\nu\beta\beta$ at the level of prospective experimental sensitivity would be the exchange of a light Majorana neutrino, leading to eq.(4), and allowing one to extract $\langle m_{\beta\beta}\rangle$ from the decay rate.

In general, however, the two scales may be distinct, as in SUSY-GUT [33] or SUSY see-saw [36] models. In these scenarios, both the Majorana neutrino mass as well as LFV effects are generated at the GUT scale. The effects of heavy Majorana neutrino exchange in $0\nu\beta\beta$ are, thus, highly suppressed. In contrast, the effects of GUT-scale LFV are transmitted to the TeV-scale by a soft SUSY-breaking sector without mass suppression via renormalization group running of the high-scale LFV couplings. Consequently, such scenarios could lead to observable effects in the upcoming LFV experiments but with an $\mathcal{O}(\alpha)$ suppression of the branching ratio $B_{\mu\to e}$ relative to $B_{\mu\to e\gamma}$ due to the exchange of a virtual photon in the conversion process rather than the emission of a real one.

As a specific example let us quote the SUSY SU(5) scenario where [37]

$$B_{\mu\to e\gamma} = 2.4 \times 10^{-12} \left(\frac{|V_{ts}|}{0.04}\frac{|V_{td}|}{0.01}\right)^2 \left(\frac{100\text{GeV}}{m_{\tilde{\mu}}}\right)^4 \ , \tag{10}$$

$$B_{\mu\to e} = 5.8 \times 10^{-12}\alpha \left(\frac{|V_{ts}|}{0.04}\frac{|V_{td}|}{0.01}\right)^2 \left(\frac{100\text{GeV}}{m_{\tilde{\mu}}}\right)^4 \ , \tag{11}$$

where the gaugino masses were neglected.

([2]) Even though the MECO experiment, that aimed at substantial incerase in sensitivity of the $\mu \to e$ conversion, was recently cancelled, proposals for experiments with similar sensitivity exist elsewhere.

Another example is the evaluation of the ratio $\mathcal{R} = B_{\mu\to e}/B_{\mu\to e\gamma}$ in the constrained seesaw minimal supersymmetric model [34] with very high scale LNV and $\mathcal{R} \sim 1/200$ for a variety of input parameters. There are, however, exceptions, like the recent evaluation of $\mathcal{R}$ in a variety of SUSY SO(10) models [35] with high scale LNV but with $\mathcal{R}$ as large as 0.3 in one case.

The case where the scales of LNV and LFV are both relatively low ($\sim$ TeV) is more subtle and requires more detailed analysis. This is the scenario which might lead to observable signals in LFV searches and at the same time generate ambiguities in interpreting a positive signal in $0\nu\beta\beta$. This is the case where one needs to develop some discriminating criteria.

Denoting the new physics scale by Λ, one has a LNV effective lagrangian (dimension $d = 9$ operators) of the form

$$\mathcal{L}_{0\nu\beta\beta} = \sum_i \frac{\tilde{c}_i}{\Lambda^5}\, \tilde{O}_i \qquad \tilde{O}_i = \bar{q}\Gamma_1 q\ \ \bar{q}\Gamma_2 q\, \bar{e}\Gamma_3 e^c\ , \tag{12}$$

where we have suppressed the flavor and Dirac structures (a complete list of the dimension nine operators $\tilde{O}_i$ can be found in Ref. [25]).

For the LFV interactions (dimension $d = 6$ operators), one has

$$\mathcal{L}_{\rm LFV} = \sum_i \frac{c_i}{\Lambda^2}\, O_i\ , \tag{13}$$

and a complete operator basis can be found in Refs.[38, 39]. The LFV operators relevant to our analysis are of the following type (along with their analogues with $L \leftrightarrow R$):

$$\begin{aligned} O_{\sigma L} &= \frac{e}{(4\pi)^2}\overline{\ell_{iL}}\,\sigma_{\mu\nu} i\not{D}\,\ell_{jL}\ F^{\mu\nu} + \text{h.c.} \\ O_{\ell L} &= \overline{\ell_{iL}}\,\ell^c_{jL}\ \overline{\ell^c_{kL}}\,\ell_{mL} \\ O_{\ell q} &= \overline{\ell_i}\Gamma_\ell \ell_j\ \bar{q}\Gamma_q q\ . \end{aligned} \tag{14}$$

Operators of the type O_σ are typically generated at one-loop level, hence our choice to explicitly display the loop factor $1/(4\pi)^2$. On the other hand, in a large class of models, operators of the type O_ℓ or $O_{\ell q}$ are generated by tree level exchange of heavy degrees of freedom. With the above choices, all non-zero c_i are nominally of the same size, typically the product of two Yukawa-like couplings or gauge couplings (times flavor mixing matrices).

With the notation established above, the ratio $\mathcal{R}$ of the branching ratios $\mu \to e$ to $\mu \to e+\gamma$ can be written schematically as follows (neglecting flavor indices in the effective couplings and the term with $L \leftrightarrow R$) [28]:

$$\begin{aligned} \mathcal{R} = \frac{\Phi}{48\pi^2} \Big| &\lambda_1\, e^2 c_{\sigma L} + e^2\,(\lambda_2 c_{\ell L} + \lambda_3 c_{\ell q}) \log\frac{\Lambda^2}{m_\mu^2} \\ &+ \lambda_4 (4\pi)^2 c_{\ell q}\ + \ldots \Big|^2 / \left[e^2\left(|c_{\sigma L}|^2 + |c_{\sigma R}|^2\right)\right]\ . \end{aligned} \tag{15}$$

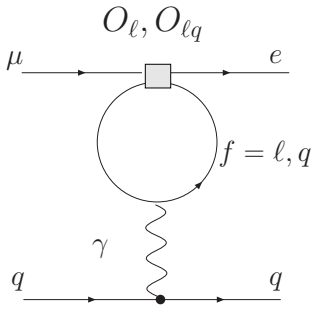

Fig. 7. – Loop contributions to $\mu \to e$ conversion through insertion of operators O_ℓ or $O_{\ell q}$, generating the large logarithm.

In the above formula $\lambda_{1,2,3,4}$ are numerical factors of $O(1)$, while the overall factor $\frac{\Phi}{48\pi^2}$ arises from phase space and overlap integrals of electron and muon wavefunctions in the nuclear field. For light nuclei $\Phi = (ZF_p^2)/(g_V^2 + 3g_A^2) \sim O(1)$ ($g_{V,A}$ are the vector and axial nucleon form factors at zero momentum transfer, while F_p is the nuclear form factor at $q^2 = -m_\mu^2$ [39]). The dots indicate subleading terms, not relevant for our discussion, such as loop-induced contributions to c_ℓ and $c_{\ell q}$ that are analytic in external masses and momenta. In contrast the logarithmically-enhanced loop contribution given by the second term in the numerator of $\mathcal{R}$ plays an essential role. This term arises whenever the operators $O_{\ell L,R}$ and/or $O_{\ell q}$ appear at tree-level in the effective theory and generate one-loop renormalization of $O_{\ell q}$ [38] (see Fig. 7).

The ingredients in eq. (15) lead to several observations: (i) In absence of tree-level $c_{\ell L}$ and $c_{\ell q}$, one obtains $\mathcal{R} \sim (\Phi\, \lambda_1^2\, \alpha)/(12\pi) \sim 10^{-3} - 10^{-2}$, due to gauge coupling and phase space suppression. (ii) When present, the logarithmically enhanced contributions, i.e. when either $c_{\ell L}$ or $c_{\ell q}$ or both are nonvanishing, compensate for the gauge coupling and phase space suppression, leading to $\mathcal{R} \sim O(1)$. (iii) If present, the tree-level coupling $c_{\ell q}$ dominates the $\mu \to e$ rate leading to $\mathcal{R} \gg 1$.

Thus, we can formulate our main conclusions regarding the discriminating power of the ratio $\mathcal{R}$:

1. Observation of both the LFV muon processes $\mu \to e$ and $\mu \to e\gamma$ with relative ratio $\mathcal{R} \sim 10^{-2}$ implies, under generic conditions, that $\Gamma_{0\nu\beta\beta} \sim \langle m_{\beta\beta} \rangle^2$. Hence the relation of the $0\nu\beta\beta$ lifetime to the absolute neutrino mass scale is straightforward.

2. On the other hand, observation of LFV muon processes with relative ratio $\mathcal{R} \gg 10^{-2}$ could signal non-trivial LNV dynamics at the TeV scale, whose effect on $0\nu\beta\beta$ has to be analyzed on a case by case basis. Therefore, in this scenario no definite conclusion can be drawn based on LFV rates.

3. Non-observation of LFV in muon processes in forthcoming experiments would imply either that the scale of non-trivial LFV and LNV is above a few TeV, and thus

$\Gamma_{0\nu\beta\beta} \sim \langle m_{\beta\beta}\rangle^2$, or that any TeV-scale LNV is approximately flavor diagonal (this is an important caveat).

The above statements are illustrated using two explicit cases[28]: the minimal supersymmetric standard model (MSSM) with R-parity violation (RPV-SUSY) and the Left-Right Symmetric Model (LRSM). Limits on the rate of the $0\nu\beta\beta$ decay were used in the past to constrain parameters of these two models [24].

RPV SUSY — If one does not impose R-parity conservation [$R = (-1)^{3(B-L)+2s}$], the MSSM superpotential includes, in addition to the standard Yukawa terms, lepton and baryon number violating interactions, compactly written as (see, e.g. [40])

$$\begin{aligned} W_{RPV} = {} & \lambda_{ijk} L_i L_j E^c_k + \lambda'_{ijk} L_i Q_j D^c_k + \lambda''_{ijk} U^c_i D^c_j D^c_k \\ & + \mu'_i L_i H_u \ , \end{aligned} \tag{16}$$

where L and Q represent lepton and quark doublet superfields, while E^c, U^c, D^c are lepton and quark singlet superfields. The simultaneous presence of λ' and λ'' couplings would lead to an unacceptably large proton decay rate (for SUSY mass scale $\Lambda_{SUSY} \sim$ TeV), so we focus on the case of $\lambda'' = 0$ and set $\mu' = 0$ without loss of generality. In such case, lepton number is violated by the remaining terms in W_{RPV}, leading to short distance contributions to $0\nu\beta\beta$ [see Fig. 8(a)], with typical coefficients [cf. eq. (12)]

$$\frac{\tilde{c}_i}{\Lambda^5} \sim \frac{\pi\alpha_s}{m_{\tilde{g}}} \frac{\lambda'^2_{111}}{m^4_{\tilde{f}}} \, ; \, \frac{\pi\alpha_2}{m_\chi} \frac{\lambda'^2_{111}}{m^4_{\tilde{f}}} \ , \tag{17}$$

where α_s, α_2 represent the strong and weak gauge coupling constants, respectively. The RPV interactions also lead to lepton number conserving but lepton flavor violating operators [see Fig. 8(b)], with coefficients [cf. eq. (13)]

$$\begin{aligned} \frac{c_\ell}{\Lambda^2} &\sim \frac{\lambda_{i11}\lambda^*_{i21}}{m^2_{\tilde{\nu}_i}}, \frac{\lambda^*_{i11}\lambda_{i12}}{m^2_{\tilde{\nu}_i}} \ , \\ \frac{c_{\ell q}}{\Lambda^2} &\sim \frac{\lambda'^*_{11i}\lambda'_{21i}}{m^2_{\tilde{d}_i}}, \frac{\lambda'^*_{1i1}\lambda'_{2i1}}{m^2_{\tilde{u}_i}} \ , \\ \frac{c_\sigma}{\Lambda^2} &\sim \frac{\lambda\lambda^*}{m^2_{\tilde{\ell}}}, \frac{\lambda'\lambda'^*}{m^2_{\tilde{q}}} \ , \end{aligned} \tag{18}$$

where the flavor combinations contributing to c_σ can be found in Ref. [41]. Hence, for generic flavor structure of the couplings λ and λ' the underlying LNV dynamics generate both short distance contributions to $0\nu\beta\beta$ and LFV contributions that lead to $\mathcal{R} \gg 10^{-2}$.

Existing limits on rare processes strongly constrain combinations of RPV couplings, assuming Λ_{SUSY} is between a few hundred GeV and ~ 1 TeV. Non-observation of LFV at future experiments MEG and MECO could be attributed either to a larger Λ_{SUSY} ($>$ few TeV) or to suppression of couplings that involve mixing among first and second generations. In the former scenario, the short distance contribution to $0\nu\beta\beta$ does not

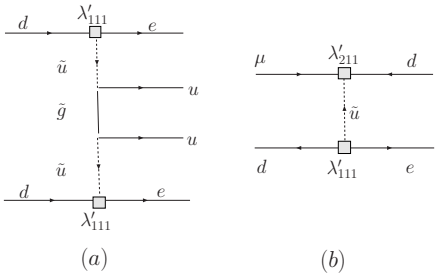

Fig. 8. – Gluino exchange contribution to $0\nu\beta\beta$ (a), and typical tree-level contribution to $O_{\ell q}$ (b) in RPV SUSY.

compete with the long distance one [see eq. (8)], so that $\Gamma_{0\nu\beta\beta} \sim \langle m_{\beta\beta}\rangle^2$. On the other hand, there is an exception to this "diagnostic tool". If the λ and λ' matrices are nearly flavor diagonal, the exchange of superpartners may still make non-negligible contributions to $0\nu\beta\beta$ without enhancing the ratio $\mathcal{R}$.

LRSM — The LRSM provides a natural scenario for introducing non-sterile, right-handed neutrinos and Majorana masses [42]. The corresponding electroweak gauge group $SU(2)_L \times SU(2)_R \times U(1)_{B-L}$, breaks down to $SU(2)_L \times U(1)_Y$ at the scale $\Lambda \geq \mathcal{O}(\text{TeV})$. The symmetry breaking is implemented through an extended Higgs sector, containing a bi-doublet Φ and two triplets $\Delta_{L,R}$, whose leptonic couplings generate both Majorana neutrino masses and LFV involving charged leptons:

$$\begin{aligned}\mathcal{L}_Y^{\text{lept}} = &- \overline{L_L}^{\,i} \left(y_D^{ij}\, \Phi \;+\; \tilde{y}_D^{ij}\, \tilde{\Phi} \right) L_R^j \\ &- \overline{(L_L)^c}^{\,i}\; y_M^{ij}\, \tilde{\Delta}_L \; L_L^j \;-\; \overline{(L_R)^c}^{\,i}\; y_M^{ij}\, \tilde{\Delta}_R \; L_R^j \; .\end{aligned} \tag{19}$$

Here $\tilde{\Phi} = \sigma_2 \Phi^* \sigma_2$, $\tilde{\Delta}_{L,R} = i\sigma_2 \Delta_{L,R}$, and leptons belong to two isospin doublets $L^i_{L,R} = (\nu^i_{L,R}, \ell^i_{L,R})$. The gauge symmetry is broken through the VEVs $\langle \Delta^0_R \rangle = v_R$, $\langle \Delta^0_L \rangle = 0$, $\langle \Phi \rangle = \text{diag}(\kappa_1, \kappa_2)$. After diagonalization of the lepton mass matrices, LFV arises from both non-diagonal gauge interactions and the Higgs Yukawa couplings. In particular, the $\Delta_{L,R}$-lepton interactions are not suppressed by lepton masses and have the structure $\mathcal{L} \sim \Delta^{++}_{L,R}\, \overline{\ell^c_i}\, h_{ij}\, (1 \pm \gamma_5) \ell_j + \text{h.c.}$. The couplings h_{ij} are in general non-diagonal and related to the heavy neutrino mixing matrix [43].

Short distance contributions to $0\nu\beta\beta$ arise from the exchange of both heavy νs and $\Delta_{L,R}$ (see Fig. 9)(a), with

$$\frac{\tilde{c}_i}{\Lambda^5} \sim \frac{g_2^4}{M^4_{W_R}} \frac{1}{M_{\nu_R}} \,;\, \frac{g_2^3}{M^3_{W_R}} \frac{h_{ee}}{M^2_\Delta} \;, \tag{20}$$

where g_2 is the weak gauge coupling. LFV operators are also generated through non-

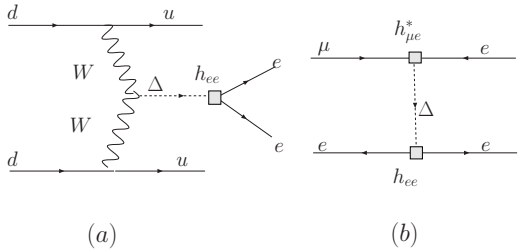

Fig. 9. – Typical doubly charged Higgs contribution to $0\nu\beta\beta$ (a) and to O_ℓ (b) in the LRSM.

diagonal gauge and Higgs vertices, with [43] (see Fig. 9(b))

$$\frac{c_\ell}{\Lambda^2} \sim \frac{h_{\mu i} h^*_{ie}}{m^2_\Delta} \qquad \frac{c_\sigma}{\Lambda^2} \sim \frac{(h^\dagger h)_{e\mu}}{M^2_{W_R}} \quad i = e, \mu, \tau \ . \tag{21}$$

Note that the Yukawa interactions needed for the Majorana neutrino mass necessarily imply the presence of LNV and LFV couplings h_{ij} and the corresponding LFV operator coefficients c_ℓ, leading to $\mathcal{R} \sim O(1)$. Again, non-observation of LFV in the next generation of experiments would typically push Λ into the multi-TeV range, thus implying a negligible short distance contribution to $0\nu\beta\beta$. As with RPV-SUSY, this conclusion can be evaded by assuming a specific flavor structure, namely y_M approximately diagonal or a nearly degenerate heavy neutrino spectrum.

In both of these phenomenologically viable models that incorporate LNV and LFV at low scale ($\sim$ TeV), one finds $\mathcal{R} \gg 10^{-2}$ [38, 41, 43]. It is likely that the basic mechanism at work in these illustrative cases is generic: low scale LNV interactions ($\Delta L = \pm 1$ and/or $\Delta L = \pm 2$), which in general contribute to $0\nu\beta\beta$, also generate sizable contributions to $\mu \to e$ conversion, thus enhancing this process over $\mu \to e\gamma$.

In conclusion of this section, the above considerations suggest that the ratio $\mathcal{R} = B_{\mu\to e}/B_{\mu\to e\gamma}$ of muon LFV processes will provide important insight about the mechanism of neutrinoless double beta decay and the use of this process to determine the absolute scale of neutrino mass. Assuming observation of LFV processes in forthcoming experiments, if $\mathcal{R} \sim 10^{-2}$ the mechanism of $0\nu\beta\beta$ is light Majorana neutrino exchange and, therefore, $1/T_{1/2} \sim \langle m_{\beta\beta}\rangle^2$; on the other hand, if $\mathcal{R} \gg 10^{-2}$, there might be TeV scale LNV dynamics, and no definite conclusion on the mechanism of $0\nu\beta\beta$ decay can be drawn based only on LFV processes.

3. – Overview of the experimental status of the search for $\beta\beta$ decay

Before embarking on the discussion of the nuclear structure aspects of the $\beta\beta$ decay let us briefly describe the experimental status of the field (more detailed information on this topics are in the lectures by A. Giuliani). The topic has a venerable history. The rate of the $2\nu\beta\beta$ decay was first estimated by Maria Goeppert-Meyer already in 1937

in her thesis work suggested by E. Wigner, basically correctly. Yet, first experimental observation in a laboratory experiment was achieved only in 1987, fifty years later [44]. (Note that this is not really exceptional in neutrino physics. It took more than twenty years since the original suggestion of Pauli to show that neutrinos are real particles in the pioneering experiment by Raines and Cowan. And it took another almost fifty years since that time to show that neutrinos are massive fermions.) Why it took so long in the case of the $\beta\beta$ decay? As pointed out above, the typical half-life of the $2\nu\beta\beta$ decay is $\sim 10^{20}$ years. Yet, its "signature" is very similar to natural radioactivity, present to some extent everywhere, and governed by the half-life of $\sim 10^{10}$ years or much less for most of the man-made or cosmogenic radioactivities. So, background suppression is the main problem to overcome when one wants to study either of the $\beta\beta$ decay modes.

During the last two decades the $2\nu\beta\beta$ decay has been observed in "live" laboratory experiments in many nuclei, often by different groups and using different methods. That shows not only the ingenuity of the experimentalists who were able to overcome the background nemesis, but makes it possible at the same time to extract the corresponding 2ν nuclear matrix element from the measured decay rate. In the 2ν mode the half-life is given by

$$1/T_{1/2} = G^{2\nu}(Q,Z)|M^{2\nu}|^2 \ , \tag{22}$$

where $G^{2\nu}(Q,Z)$ is an easily and accurately calculable phase space factor.

The resulting nuclear matrix elements $M^{2\nu}$, which have the dimension energy^{-1}, are plotted in Fig.10. Note the pronounced shell dependence; the matrix element for ^{100}Mo is almost ten times larger than the one for ^{130}Te. Evaluation of these matrix elements, to be discussed below, is an important test for the nuclear theory models that aim at the determination of the analogous but different quantities for the 0ν neutrinoless mode.

The challenge of detecting the $0\nu\beta\beta$ decay is, at first blush, easier. Unlike the continuous $2\nu\beta\beta$ decay spectrum with a broad maximum at rather low energy where the background suppression is harder, the $0\nu\beta\beta$ decay spectrum is sharply peaked at the known Q value (see Fig.3), at energies that are not immune to the background, but a bit less difficult to manage. However, as also indicated in Fig.3, to obtain interesting results at the present time means to reach sensitivity to the 0ν half-lives that are $\sim 10^6$ times longer than the 2ν decay half-life of the same nucleus.

The historical lessons are illustrated in Fig.11 where the past limits on the $0\nu\beta\beta$ decay half-lives of various candidate nuclei are translated using eq.(4) into the limits on the effective mass $\langle m_{\beta\beta}\rangle$. When plotted in the semi-log plot this figure represent "Moore's law" of double beta decay, and indicates that, provided that the past trend will continue, the mass scale corresponding to Δm^2_{atm} will be reached in about 7 years. This is also the time scale of significant experiments these days. Note that the figure was made using some assumed values of the corresponding nuclear matrix elements, without including their uncertainty. For such illustrative purposes they are, naturally, irrelevant.

The past search for the neutrinoless double beta decay, illustrated in Fig.11, was driven by the then current technology and the resources of the individual experiments.

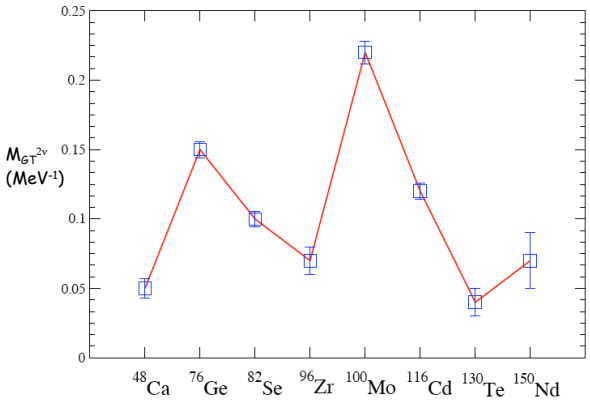

Fig. 10. – Nuclear matrix elements for the $2\nu\beta\beta$ decay extracted from the measured half-lives.

The goal has been simply to reach sensitivity to longer and longer half-lives. The situation is different, however, now. The experimentalists at the present time can, and do, use the knowledge summarized in Fig. 5 to gauge the aim of their proposals. Based on that figure, the range of the mass parameter $\langle m_{\beta\beta}\rangle$ can be divided into three regions of interest.

- The degenerate mass region where all $m_i \gg \sqrt{\Delta m^2_{atm}}$. In that region $\langle m_{\beta\beta}\rangle \geq 0.1$ eV, corresponding crudely to the 0ν half-lives of 10^{26-27} years. To explore it (in a realistic time frame), $\sim$ 100 kg of the decaying nucleus is needed. Several experiments aiming at such sensitivity are being built and should run very soon and give results within the next $\sim$ 3 years. Moreover, this mass region (or a substantial part of it) will be explored, in a similar time frame, by the study of ordinary β decay (in particular of tritium, see the lectures by C. Weinheimer) and by the observational cosmology (see the lectures by S. Pastor). These techniques are independent on the Majorana nature of neutrinos. It is easy, but perhaps premature, to envision various possible scenarios depending on the possible outcome of these measurements.

- The so-called inverted hierarchy mass region where $20 < \langle m_{\beta\beta}\rangle < 100$ meV and the $0\nu\beta\beta$ half-lives are about 10^{27-28} years. (The name is to some extent a misnomer. In that interval one could encounter not only the inverted hierarchy but also a quasi-degenerate but normal neutrino mass ordering. Successfull observation of the $0\nu\beta\beta$ decay will not be able to distinguish these possibilities, as I argued above. This is so not only due to the anticipated experimental accuracy, but more fundamentally due to the unknown Majorana phases.) To explore this mass region, $\sim$ ton size

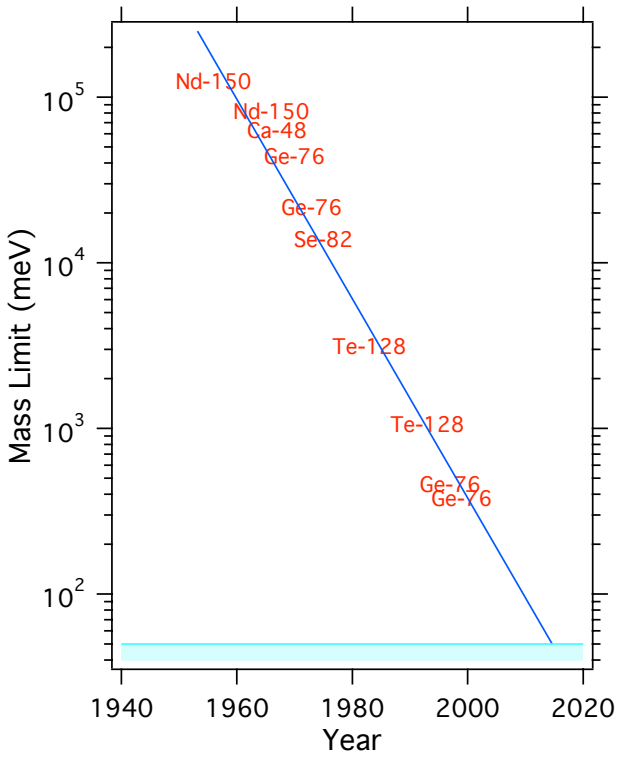

Fig. 11. – The limit of the effective mass $\langle m_{\beta\beta}\rangle$ extracted from the experimental lower limits on the $0\nu\beta\beta$ decay half-life versus the corresponding year. The gray band near bottom indicates the $\sqrt{\Delta m^2_{atm}}$ value. Figure originally made by S. Elliott.

sources would be required. Proposals for the corresponding experiments exist, but none has been funded as yet, and presumably the real work will begin depending on the experience with the various $\sim$ 100 kg size sources. Timeline for exploring this mass region is $\sim$ 10 years.

- Normal mass hierarchy region where $\langle m_{\beta\beta}\rangle \leq$ 10-20 meV. To explore this mass region, $\sim$ 100 ton sources would be required. There are no realistic proposals for experiments of this size at present.

Over the last two decades, the methodology for double beta decay experiments has improved considerably. Larger amounts of high-purity enriched parent isotopes, combined with careful selection of all surrounding materials and using deep-underground sites have lowered backgrounds and increased sensitivity. The most sensitive experiments to date use ^{76}Ge, ^{100}Mo, ^{116}Cd, ^{130}Te, and ^{136}Xe. For ^{76}Ge the lifetime limit reached impressive values exceeding 10^{25}years[45, 46]. The experimental lifetime limits have been interpreted to yield effective neutrino mass limits typically a few eV and in

^{76}Ge as low as 0.3 - 1.0 eV (the spread reflects an estimate of the uncertainty in the nuclear matrix elements). Similar sensitivity to the neutrino mass was reached recently also in the CUORICINO experiment with ^{130}Te [47].

While all these experiments reported lower limits on the $0\nu\beta\beta$-decay half-lives, a subset of members of the Heidelberg-Moscow collaboration [48] reanalyzed the data (and used additional information, e.g. the pulse-shape analysis and a different algorithm in the peak search) and claimed to observe a positive signal corresponding, in the latest publication, to the half-life $T_{1/2} = 2.23^{+0.44}_{-0.31} \times 10^{25}$ years. That report has been followed by a lively discussion. Clearly, such an extraordinary claim with its profound implications, requires extraordinary evidence. It is fair to say that a confirmation, both for the same ^{76}Ge parent nucleus, and better yet also in another nucleus with a different Q value, would be required for a consensus. In any case, if that claim is eventually confirmed (and the mechanism of the $0\nu\beta\beta$ decay determined, i.e. the validity of eq. (4) assured), the degenerate mass scenario will be implicated, and eventual positive signal in the analysis of the tritium β decay and/or observational cosmology should be forthcoming. For the neutrinoless $\beta\beta$ decay the next generation of experiments, which will use $\sim$ 100 kg of decaying isotopes will, among other things, test this recent claim.

4. – Basic nuclear physics of $\beta\beta$ decay

Whether a nucleus is stable or undergoes weak decay is determined by the dependence of the atomic mass M_A of the isotope (Z, A) on the nuclear charge Z. This functional dependence near its minimum can be approximated by a parabola

$$M_A(Z,A) \;=\; const \;+\; 2b_{sym}\frac{(A/2-Z)^2}{A^2} \;+\; b_{Coul}\frac{Z^2}{A^{1/3}} \;+\; m_e Z \;+\; \delta \;, \tag{23}$$

where the symmetry energy coefficient is $b_{sym} \sim 50$ MeV and the Coulomb energy coefficient is $b_{Coul} \sim 0.7$ MeV. The $m_e Z$ term represents the mass of the bound electrons; their binding energy, for our purposes, is small enough to be neglected. The last term δ, decisive for the application to the $\beta\beta$ decay, describes nuclear pairing, the increase in binding as pairs of like nucleons couple to angular momentum zero. It is a small correction term and is given in a crude approximation by $\delta \sim \pm 12/A^{1/2}$ MeV for odd N and odd Z, or even N and even Z, respectively, while $\delta = 0$ for odd A. Thus, for odd A nuclei, typically only one isotope is stable; nuclei with charge Z smaller than the stable nucleus decay by electron emission, while those with larger Z decay by electron capture or positron emission or by both these modes simultaneously. For even A nuclei the situation is different. Due to the pairing term δ, the even-even nuclei form one parabola while the odd-odd nuclei form another one, at larger mass, as shown in Fig. 2, using A = 136 as an example. Consequently, in a typical case there exist two (or three as in Fig. 2) even-even nuclei for a given A which are stable against both electron and positron (or EC) decays. As these nuclei usually do not have the same mass, the heavier may decay into the lighter through a second order weak process in which the nuclear charge changes by two units. This process is double beta decay. In Fig. 12 all nuclei that are practical

	Q (MeV)	Abund.(%)
$^{48}Ca \rightarrow ^{48}Ti$	4.271	0.187
$^{76}Ge \rightarrow ^{76}Se$	2.040	7.8
$^{82}Se \rightarrow ^{82}Kr$	2.995	9.2
$^{96}Zr \rightarrow ^{96}Mo$	3.350	2.8
$^{100}Mo \rightarrow ^{100}Ru$	3.034	9.6
$^{110}Pd \rightarrow ^{110}Cd$	2.013	11.8
$^{116}Cd \rightarrow ^{116}Sn$	2.802	7.5
$^{124}Sn \rightarrow ^{124}Te$	2.228	5.64
$^{130}Te \rightarrow ^{130}Xe$	2.533	34.5
$^{136}Xe \rightarrow ^{136}Ba$	2.479	8.9
$^{150}Nd \rightarrow ^{150}Sm$	3.367	5.6

Fig. 12. – Candidate nuclei for $\beta\beta$ decay with $2e^-$ emission and with the Q value >2 MeV. The corresponding abundances are also shown.

candidates for the search for the $0\nu\beta\beta$ decay are listed. All of them exist in nature since their lifetime is longer than the age of the solar system. However, with a single exception (^{130}Te), all of them are relatively rare so that a large scale experiments also require a large scale and costly (and sometimes technically difficult) isotope enrichment.

Double beta decay, therefore, proceeds between two even-even nuclei. All ground states of even-even nuclei have spin and parity 0^+ and thus transitions $0^+ \rightarrow 0^+$ are expected in all cases. Occasionally, population of the low-lying excited states of the daughter nucleus is energetically possible, giving rise to $0^+ \rightarrow 2^+$ transitions or to transitions to the excited 0^+ states.

Double beta decay with the electron emission (both the 2ν and 0ν modes) in which the nuclear charge increases by two units is subject to the obvious condition

$$M_A(Z,A) > M_A(Z+2,A)\ , \quad \text{while} \quad M_A(Z,A) < M_A(Z+1,A)\ , \tag{24}$$

where M_A is the *atomic mass*, with the supplementary practical requirement that single beta decay is absent, or that it is so much hindered (e.g., by the angular momentum selection rules) that it does not compete with double beta decay.

Double beta decay with the positron emission and/or electron capture (both the 2ν and 0ν modes) in which the nuclear charge decreases by two units can proceed in three different ways:

- Two positron emission when $M_A(Z,A) > M_A(Z-2,A) + 4m_e$,
- One positron emission and one electron capture when $M_A(Z,A) > M_A(Z-2,A) + 2m_e + B_e$, and

- Two electron captures (only the two neutrino mode, see below for the comment on the 0ν mode) when $M_A(Z,A) > M_A(Z-2,A) + B_e(1) + B_e(2)$,

where B_e is the positive binding energy of the captured electron. As mentioned above, a complete list of all candidate nuclei (except the double electron capture) with the corresponding phase space factors for both $\beta\beta$-decay modes is given in Ref.[23].

Since the relevant masses are atomic masses, the processes with emission of positrons have reduced phase space (terms with m_e above). While from the point of view of experimental observation the positron emission seems advantageous (possibility to observe the annihilation radiation), the reduction of phase space means that the corresponding lifetimes are quite long. In fact, not a single such decay has been observed so far.

The two electron capture decay without neutrino emission requires a special comment. Clearly, when the initial and final states have different energies, the process cannot proceed since energy is not conserved. The radiative process, with bremsstrahlung photon emission, however, can proceed and its rate, unlike all the other neutrinoless processes, increases with decreasing Q value [49]. (However, the estimated decay rates are quite small and lifetimes long). In the extreme case of essentially perfect degeneracy, a resonance enhancement can occur [50].

The case of resonance, though probably unrealistic, perhaps deserves some explanations. The initial state is the atom (Z,A), stable against ordinary β decay. The final state is the ion $(Z-2,A)$ with electron vacancies H, H' and, in general, with the nucleus in some excited state of energy E^*. The resonance occurs if the final energy

$$E = E^* + E_H + E_{H'} \tag{25}$$

is close to the decay Q value, i.e. the difference of the initial and final atomic masses, and a perfect resonance occurs when $Q - E$ is less than the width of the final state which is dominated by the electron hole widths $\Gamma_H, \Gamma_{H'}$. The decay rate near resonance is given by the Breit-Wigner type formula

$$\frac{1}{\tau} = \frac{(\Delta M)^2}{(Q-E)^2 + \Gamma^2/4}\Gamma \ , \tag{26}$$

where ΔM is the matrix element of weak interaction between the two degenerate atomic states.

The states of definite energy, the eigenstates of the total hamiltonian, are superpositions of the initial and final states, mixed by ΔM. But in reality, the initial state is pure, and not a state of definite energy, since the final state decays essentially immediately.

The mixing matrix element is [50]

$$\Delta M \sim \frac{G_F^2 \cos^2\theta_C}{4\pi}\langle m_{\beta\beta}\rangle |\psi(0)|^2 g_A^2 M^{0\nu} \ , \tag{27}$$

where $\psi(0)$ is the amplitude at the origin of the wave function of the captured electrons and $M^{0\nu}$ is the nuclear matrix element discussed later. Clearly, if the resonance can be

approached, the decay rate would be enhanced by the factor $4/\Gamma$ compared to $\Gamma/(E-Q)^2$, where the width Γ is typically tens of eV. Estimates suggest that in such a case the decay lifetime for $\langle m_{\beta\beta}\rangle \sim 1$ eV could be of the order of 10^{24-25} years, competitive to the rate with $2e^-$ emission. However, chances of finding a case of a perfect (eV size) resonance when E is of order of MeV are very unlikely.

5. – Decay rate formulae

5˙1. 2ν *decay.* – Even though the $2\nu\beta\beta$-decay mode is unrelated to the fundamental particle physics issues, it is worthwhile to discuss it in some detail. This is so because it is the mode that is actually seen experimentally; it is also the inevitable background for the $0\nu\beta\beta$-decay mode. In nuclear structure theory the corresponding rate is used as a test of the adequacy of the corresponding nuclear models. And various auxiliary experiments can be performed to facilitate the evaluation of the $M^{2\nu}$ nuclear matrix elements.

The derivation of the $2\nu\beta\beta$-decay rate formula is analogous to the treatment of ordinary beta decay. It begins with the Fermi golden rule for second order weak decay

$$\frac{1}{\tau} = 2\pi\delta(E_0 - \Sigma_f E_f)\left[\Sigma_{m,\beta}\frac{\langle f|H_\beta|m\rangle\langle m|H^\beta|i\rangle}{E_i - E_m - p_\nu - E_e}\right]^2 , \tag{28}$$

where the sum over m includes all relevant virtual states in the intermediate odd-odd nucleus and β labels the different Dirac structures of the weak interaction Hamiltonian. Next we take into account that the weak Hamiltonian is the product of the nuclear and lepton currents; the corresponding formula will include the summation over the indeces of the emitted leptons. Then the summation over the lepton polarizations is performed, taking into account the indistinguishability of the final lepton pairs. Because we are interested in the rate formula, we neglect terms linear in $\vec{p}_e$ and $\vec{p}_\nu$ that disappear after integration over angles. (The angular distribution of the electrons is of the form (1 - $\vec{\beta}_1 \cdot \vec{\beta}_2$) for the $0^+ \to 0^+$ transitions, where $\vec{\beta}_i$ is the velocity of the electron i).

The energy denominators are of the following form

$$K_m(M_m) = \frac{1}{E_m - E_i + p_{\nu 1} + E_{e1}} \pm \frac{1}{E_m - E_i + p_{\nu 2} + E_{e2}} , \tag{29}$$

where the + sign belongs to K_m and the − sign to M_m and

$$L_m(N_m) = \frac{1}{E_m - E_i + p_{\nu 2} + E_{e1}} \pm \frac{1}{E_m - E_i + p_{\nu 1} + E_{e2}} . \tag{30}$$

The energy denominators in the factors $K,\ M,\ L,\ N$ contain contributions of the nuclear energies $E_m - E_i$, as well as the lepton energies $E_e + p_\nu$. When calculating the $0^+ \to 0^+$ transitions, it is generally a very good approximation to replace these lepton energies by the corresponding average value, i.e., $E_e + p_\nu \sim E_0/2$, where the $E_0 = M_i - M_f$ is the

total decay energy including electron masses. In that case $M_m = N_n = 0$ and

$$K_m = L_m \sim \frac{1}{E_m - E_i + E_0/2} = \frac{1}{E_m - (M_i + M_f)/2} \ . \tag{31}$$

The lepton momenta, for both electrons and neutrinos are all $q < Q$ and thus $qR \ll 1$, where R is the nuclear radius. Hence the so-called long wavelength approximation is valid and the rate formula (with eq. (31)) separates into a product of the nuclear and lepton parts, where the lepton part contains just the phase space integral

$$\int_{m_e}^{E_0 - m_e} F(Z, E_{e1}) p_{e1} E_{e1} dE_{e1} \int_{m_e}^{E_0 - E_1} F(Z, E_{e2}) p_{e2} E_{e2} dE_{e2} (E_0 - E_{e1} - E_{e2})^5 / 30 \ , \tag{32}$$

where the integration over the neutrino momentum was already performed. The single electron spectrum is obtained by performing integration over dE_{e2}, while the spectrum of summed electron energies is obtained by changing the variables to $E_{e1} + E_{e2}$ and $E_{e1} - E_{e2}$ and performing the integration over the second variable. If an accurate result is required, the relativistic form of the function $F(Z, E)$ must be used and numerical evaluation is necessary.

For a qualitative and intuitive picture, one can use the simplified nonrelativistic Coulomb expression, so-called Primakoff-Rosen approximation [52]

$$F(Z, E) = \frac{E}{p} \frac{2\pi Z\alpha}{1 - e^{-2\pi Z\alpha}} \ . \tag{33}$$

This approximation allows us to perform the required integrals analytically.

For example, the sum electron spectrum, which is of primary interest from the experimental point of view is then independent of Z,

$$\frac{dN}{dK} \sim K(T_0 - K)^5 \left(1 + 2K + \frac{4K^2}{3} + \frac{K^3}{3} + \frac{K^4}{30} \right) \ , \tag{34}$$

where K is the sum of the kinetic energies of both electrons, in units of electron mass. The Coulomb effects result in shifting the maximum of dN/dK towards lower energy and in making the approach of dN/dK to zero when $K \to T_0$ steeper.

The nuclear structure information is contained in the nuclear matrix element; only the Gamow-Teller $\sigma\tau$ part contributes in the long wavelength approximation

$$M^{2\nu} = \Sigma_m \frac{\langle 0_f^+ | \vec{\sigma}_i \tau_i^+ | m \rangle \langle m | \vec{\sigma}_k \tau_k^+ | 0_i^+ \rangle}{E_m - (M_i + M_f)/2} \ . \tag{35}$$

The individual terms in the eq. (35) have a well defined meaning, in particular for the most relevant ground state to ground state transitions. The terms $\langle m | \vec{\sigma}_k \tau_k^+ | 0_i^+ \rangle$ represent the β^- strength in the initial nucleus and can be explored in the nucleon exchange reactions such as (p, n) and $({}^3He, t)$. On the other hand the terms $\langle 0_f^+ | \vec{\sigma}_i \tau_i^+ | m \rangle$

represent the β^+ strength in the final nucleus and can be explored in the nucleon charge exchange reactions such as (n,p) and $(d,^2He)$. In this way one can (up to the sign) explore the contribution of several low lying states to the $M^{2\nu}$ matrix element.

It turns out that in several nuclei the lowest (or few lowest) 1^+ states give a dominant contribution to $M^{2\nu}$. (This is so-called "single state dominance".) In those cases the above mentioned experiments allow one to determine the $M^{2\nu}$ indirectly, independently of the actual $2\nu\beta\beta$ decay. Such data are, naturally, a valuable testing ground of nuclear theory. On the other hand, it is not a priori clear and easy to decide in which nuclei the sum over the 1^+ states in eq. (35) converges very fast and in which nuclei many states contribute. We will return to this issue later.

Since, as stated in Section 3, the half-lives of many $2\nu\beta\beta$ decays was experimentally determined. One can then extract the values of the nuclear matrix elements $M^{2\nu}$ using eq. (35) . They are depicted in Fig. 10. For completeness, we add a table of the most recent half-life measurements of the $2\nu\beta\beta$ decay.

TABLE I. – *Summary of experimentally measured $2\nu\beta\beta$ half-lives and matrix elements, mostly from the NEMO experiment [51] (^{136}Xe is an important exception where a limit is quoted).*

Isotope	$T^{2\nu}_{1/2}$ (y)	$M^{2\nu}_{GT}$ (MeV^{-1})
^{48}Ca	$(3.9 \pm 0.7 \pm 0.6) \times 10^{19}$	0.05 ± 0.01
^{76}Ge	$(1.7 \pm 0.2) \times 10^{21}$	0.13 ± 0.01
^{82}Se	$(9.6 \pm 0.3 \pm 1.0) \times 10^{19}$	0.10 ± 0.01
^{96}Zr	$(2.0 \pm 0.3 \pm 0.2) \times 10^{19}$	0.12 ± 0.02
^{100}Mo	$(7.11 \pm 0.02 \pm 0.54) \times 10^{18}$	0.23 ± 0.01
^{116}Cd	$(2.8 \pm 0.1 \pm 0.3) \times 10^{19}$	0.13 ± 0.01
$^{128}Te^{(1)}$	$(2.0 \pm 0.1) \times 10^{24}$	0.05 ± 0.005
^{130}Te	$(7.6 \pm 1.5 \pm 0.8) \times 10^{20}$	0.032 ± 0.003
^{136}Xe	$> 1.0 \times 10^{22}$ (90% CL)	<0.01
^{150}Nd	$(9.2 \pm 0.25 \pm 0.73) \times 10^{18}$	0.06 ± 0.003
$^{238}U^{(2)}$	$(2.0 \pm 0.6) \times 10^{21}$	0.05 ± 0.01

$^{(1)}$deduced from the geochemically determined half-life ratio $^{128}Te/^{130}Te$
$^{(2)}$radiochemical result for all decay modes

5˙2. 0ν *rate.* – We shall now indicate the derivation of the electron spectra and decay rates associated with the nonvanishing value of m_ν. The decay rate is of the general form

$$\omega_{0\nu} = 2\pi\Sigma_{spin}|R_{0\nu}|^2\delta(E_{e1} + E_{e2} + E_f - M_i)d^3p_{e1}d^3p_{e2} \ , \tag{36}$$

where E_f is the energy of the final nucleus and $R_{0\nu}$ is the transition amplitude including both the lepton and nuclear parts.

The lepton part of the amplitude is written as a product of two left-handed currents

$$\bar{e}(x)\gamma_\rho \frac{1}{2}(1-\gamma_5)\nu_j(x)\bar{e}(y)\gamma_\sigma \frac{1}{2}(1-\gamma_5)\nu_k(y) \ , \tag{37}$$

where, ν_j, ν_k represent neutrino mass eigenstates j and k, and there is a contraction over the two neutrino operators. The contraction above is allowed only if the neutrinos are Majorana particles.

After substitution for the neutrino propagator and integration over the virtual neutrino momentum, the lepton amplitude acquires the form

$$-i\delta_{jk}\int \frac{d^4q}{(2\pi)^4}\frac{e^{-iq(x-y)}}{q^2-m_j^2}\bar{e}(x)\gamma_\rho \frac{1}{2}(1-\gamma_5)(q^\mu\gamma_\mu + m_j)\frac{1}{2}(1-\gamma_5)\gamma_\sigma e^C(y) \ . \tag{38}$$

From the commutation properties of the gamma matrices it follows that

$$\frac{1}{2}(1-\gamma_5)(q^\mu\gamma_\mu + m_j)\frac{1}{2}(1-\gamma_5) = m_j\frac{1}{2}(1-\gamma_5) \ . \tag{39}$$

Thus the decay amplitude for purely left-handed lepton currents is proportional to the neutrino Majorana mass m_j.

Integration over the virtual neutrino energy leads to the replacement of the propagator $(q^2-m_j^2)^{-1}$ by the residue π/ω_j with $\omega_j = (\vec{q}^{\,2}+m_j^2)^{1/2}$. For the remaining integration over the space part $d\vec{q}$ we have to consider, besides this denominator ω_j, the energy denominators of the second order perturbation expression. Denoting

$$A_n = E_n - E_i + E_e \ , \tag{40}$$

we find that integration over $d\vec{q}$ leads to an expression representing the effect of the neutrino propagation between the two nucleons. This expression has the form of a "neutrino potential" and appears in the corresponding nuclear matrix elements, introducing dependence of the transition operator on the coordinates of the two nucleons, as well as a weak dependence on the excitation energy $E_n - E_i$ of the virtual state in the odd-odd intermediate nucleus.

There are several neutrino potentials as explained in the next subsection. The main one is of the form

$$H(r,E_m) = \frac{R}{2\pi^2 g_A^2}\int \frac{d\vec{q}}{\omega}\frac{1}{\omega + A_m}e^{i\vec{q}\cdot\vec{r}} = \frac{2R}{\pi r g_A^2}\int_0^\infty dq \frac{q\sin(qr)}{\omega(\omega+A_m)} \ . \tag{41}$$

Here we added the nuclear radius $R = 1.2A^{1/3}$ fm as an auxiliary factor so that H becomes dimensionless. A corresponding $1/R^2$ compensates for this auxiliary quantity in the phase space formula. Note that a consistency between the definitions of the nuclear radius R is required.) The first factor ω in the denominator of eq. (41) is the residue, while the factor $\omega + A_m$ is the energy denominator of perturbation theory. To obtain the

final result one has to treat properly the antisymmetry between the identical outgoing electrons (see [53]).

The momentum of the virtual neutrino is determined by the uncertainty relation $q \sim 1/r$, where $r \leq R$ is a typical spacing between two nucleons. We will show later that in fact the relevant values of r are only $r \leq$ 2-3 fm, so that the momentum transfer $q \sim$ 100-200 MeV. For the light neutrinos the neutrino mass m_j can then be safely neglected in the potential $H(r)$. (Obviously, for heavy neutrinos, with masses $M_j \gg 1$ GeV a different procedure is necessary.) Also, given the large value of q the dependence on the difference of nuclear energies $E_m - E_i$ is expected to be rather weak and the summation of the intermediate states can be performed in closure for convenience. (We will discuss the validity of that approximation later.)

Altogether, we can rewrite the expression for the neutrino potential as

$$H(r) = \frac{R}{r}\Phi(\omega r) \ , \tag{42}$$

where $\Phi(\omega r) \leq 1$ is a relatively slowly varying function of r. From that it follows that a typical value of $H(r)$ is larger than unity, but less than 5-10. In the next subsection we present the exact expressions for the neutrino potentials and the $0\nu\beta\beta$ transition operator for the most interesting case of small but finite neutrino Majorana masses m_j.

For now we use the relation (4) and evaluate the phase space function $G^{0\nu}$

$$G^{0\nu}(Q,Z) \sim \int F(Z,E_{e1})F(Z,E_{e2})p_{e1}p_{e2}E_{e1}E_{e2}\delta(E_0 - E_{e1} - E_{e2})dE_{e1}dE_{e2} \ . \tag{43}$$

The constant factor in front of this expression is

$$(G_F \cos\theta_C g_A)^4 \left(\frac{\hbar c}{R}\right)^2 \frac{1}{\hbar}\frac{1}{\ln(2)32\pi^5} \ , \tag{44}$$

and the values of $1/G^{0\nu}$ listed in Ref. [23] are in years provided that the neutrino masses are in eV.

Again, in the Primakoff-Rosen approximation, eq. (33), $G^{0\nu}$ is independent of Z and (only the E_0 dependence is shown)

$$G^{0\nu}_{PR} \sim \left(\frac{E_0^5}{30} - \frac{2E_0^2}{3} + E_0 - \frac{2}{5}\right) \ , \tag{45}$$

where E_0 is expressed in units of electron mass. Each of the two electrons observed separately will have energy spectrum determined by the phase space integral. In the Primakoff-Rosen approximation its shape is

$$\frac{dN}{dT_e} \sim (T_e + 1)^2(T_0 - T_e + 1)^2 \ , \tag{46}$$

where again the kinetic energies are in the units of electron mass.

It is of interest to contrast the 0ν and 2ν decay modes from the point of view of the phase space integrals. The 0ν mode has the advantage of the two-lepton final state, with the characteristic E_0^5 dependence compared to the four-lepton final state with E_0^{11} dependence for the 2ν mode. In addition, the large average momentum of the virtual neutrino, compared with the typical nuclear excitation energy also makes the 0ν decay faster. Thus, if $\langle m_{\beta\beta}\rangle$ were to be of the order of m_e, the 0ν decay would be $\sim 10^5$ times faster than the 2ν decay. It is this phase space advantage which makes the $0\nu\beta\beta$ decay a sensitive probe for Majorana neutrino mass.

Finally, let us remark that it is possible that, in addition to the two electrons, a light boson, the so called majoron, is emitted. This transition would have three-body phase space, giving rise to a continuous spectrum peaked at approximately three quarters of the decay energy T_0. We shall not discuss this topic here, but refer to Doi et al. [53] for a discussion of this issue.

Also, since we concentrate on the mechanism involving the exchange of light Majorana neutrinos, we will not discuss in any detail the case of hypothetical right-handed currents.

5˙3. *Exact expressions for the transition operator*. – After the qualitative discussion in the preceding subsection, here we derive the exact expressions for the transition operator.

The hadronic current, expressed in terms of nucleon fields Ψ, is

$$J^{\rho\dagger} = \overline{\Psi}\tau^+ \left[g_V(q^2)\gamma^\rho + i g_M(q^2)\frac{\sigma^{\rho\nu}}{2m_p}q_\nu - g_A(q^2)\gamma^\rho\gamma_5 - g_P(q^2)q^\rho\gamma_5 \right] \Psi \ , \tag{47}$$

where m_p is the nucleon mass and q^μ is the momentum transfer, i.e. the momentum of the virtual neutrino. Since in the $0\nu\beta\beta$ decay $\vec{q}^{\,2} \gg q_0^2$ we take $q^2 \simeq -\vec{q}^{\,2}$.

For the vector and axial vector form factors we adopt the usual dipole approximation

$$g_V(\vec{q}^{\,2}) = g_V/(1+\vec{q}^{\,2}/M_V^2)^2, \quad g_A(\vec{q}^{\,2}) = g_A/(1+\vec{q}^{\,2}/M_A^2)^2 \ , \tag{48}$$

with $g_V = 1$, $g_A = 1.254$, $M_V = 850$ MeV, and $M_A = 1086$ MeV. These form factors are a consequence of the composite nature of nucleons. With high momentum transfer the "elastic" transitions, in which a nucleon remains nucleon and no other hadrons are produced, is reduced.

We use the usual form for the weak magnetism, and the Goldberger-Treiman relation for the induced pseudoscalar term:

$$g_M(\vec{q}^{\,2}) = (\mu_p - \mu_n) g_V(\vec{q}^{\,2}) \ , \quad g_P(\vec{q}^{\,2}) = 2m_p g_A(\vec{q}^{\,2})/(\vec{q}^{\,2} + m_\pi^2) \ . \tag{49}$$

Reducing the nucleon current to the non-relativistic form yields (see Ref.[54]):

$$J^{\rho\dagger}(\vec{x}) = \sum_{n=1}^{A} \tau_n^+ [g^{\rho 0} J^0(\vec{q}^{\,2}) + \sum_k g^{\rho k} J_n^k(\vec{q}^{\,2})] \delta(\vec{x} - \vec{r}_n), \tag{50}$$

where $J^0(\vec{q}^{\,2}) = g_V(q^2)$ and

$$\vec{J}_n(\vec{q}^{\,2}) = g_M(\vec{q}^{\,2}) i \frac{\vec{\sigma}_n \times \vec{q}}{2m_p} + g_A(\vec{q}^{\,2})\vec{\sigma} - g_P(\vec{q}^{\,2}) \frac{\vec{q}\,\vec{\sigma}_n \cdot \vec{q}}{2m_p}, \tag{51}$$

$\vec{r}_n$ is the coordinate of the nth nucleon, $k = 1, 2, 3$, and $g^{\rho,\alpha}$ is the metric tensor.

This allows us to derive the effective two-body transition operator in the momentum representation:

$$\Omega = \tau^+\tau^+ \frac{(-h_F + h_{GT}\sigma_{12} - h_T S_{12})}{q(q + E_m - (M_i + M_f)/2)} \ , \ \sigma_{12} = \vec{\sigma}_1 \cdot \vec{\sigma}_2 \ , \ S_{12} = 3\vec{\sigma}_1 \cdot \hat{q}\vec{\sigma}_2 \cdot \hat{q} - \sigma_{12} \ . \tag{52}$$

Here $h_F = g_V^2$ and

$$h_{GT} = g_A^2 \left[1 - \frac{2}{3} \frac{\vec{q}^{\,2}}{\vec{q}^{\,2} + m_\pi^2} + \frac{1}{3} \left(\frac{\vec{q}^{\,2}}{\vec{q}^{\,2} + m_\pi^2} \right)^2 \right] , \ h_T = g_A^2 \left[\frac{2}{3} \frac{\vec{q}^{\,2}}{\vec{q}^{\,2} + m_\pi^2} - \frac{1}{3} \left(\frac{\vec{q}^{\,2}}{\vec{q}^{\,2} + m_\pi^2} \right)^2 \right] . \tag{53}$$

For simplicity the q^2 dependence of the form factors g_V and g_A is not indicated and the terms containing $1/m_p^2$ are omitted. The parts containing $\vec{q}^{\,2} + m_\pi^2$ come from the induced pseudoscalar form factor g_P for which the partially conserved axial-vector hypothesis (PCAC) is used.

In order to calculate the nuclear matrix element in the coordinate space, one has to evaluate first the "neutrino potentials" that, at least in principle, depend explicitly on the energy E_m of the virtual intermediate state

$$H_K(r_{12}) = \frac{2}{\pi g_A^2} R \int_0^\infty f_K(qr_{12}) \frac{h_K(q^2) q dq}{q + E_m - (M_i + M - f)/2} \ , \tag{54}$$

where $K = F, GT, T$ and $f_{F,GT} = j_0(qr_{12})$ and $f_T = -j_2(qr_{12})$, and r_{12} is the internucleon distance.

With these "neutrino potentials" and the spin dependence given in eq. (52) where, naturally, in the tensor operator the unit vector $\hat{q}$ is replaced by $\hat{r}_{12}$, the nuclear matrix element is now written (see [72])

$$M'^{0\nu} = \left(\frac{g_A}{1.25} \right)^2 \langle f | \frac{M^{0\nu}}{g_A^2} + M_{GT}^{0\nu} + M_T^{0\nu} | i \rangle \ , \tag{55}$$

where $|f\rangle$ and $|i\rangle$ are the ground state wave functions of the final and, respectively, initial nuclei. The somewhat awkward definition of $M'^{0\nu}$ is used so that, if needed, one can use an "effective" value of the axial coupling constant g_A but still use the tabulated values of the phase space integral $G^{0\nu}$ that were evaluated with $g_A = 1,25$.

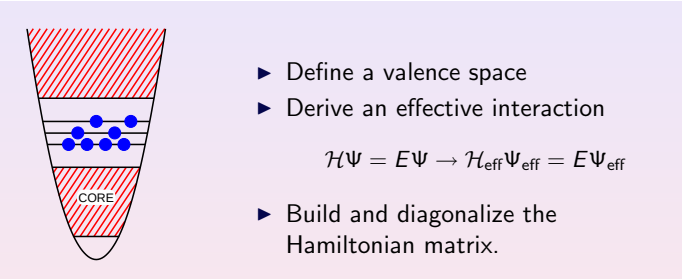

Fig. 13. – Schematic illustration of the basic procedures in the nuclear shell model.

6. – Nuclear structure issues

We will discuss now the procedures to evaluate the ground state wave functions of the initial and final nuclei $|f\rangle$ and $|i\rangle$ and the nuclear matrix element, eq. (55). There are two complementary methods to accomplish this task, the nuclear shell model (NSM) and the quasiparticle random phase approximation (QRPA). Since my own work deals with the QRPA method and the NSM will be covered by Prof. Poves in his seminar, the NSM will be described only superficially and reference to its results will be made mainly in comparison with the QRPA.

6˙1. *Nuclear shell model.* – The basic idea is schematically indicated in Fig. 13. The procedure should describe, at the same time, the energies and transition probabilities involving the low-lying nuclear states as well as the β and $\beta\beta$ decay nuclear matrix elements. The hamiltonian matrix is diagonalized in one of two possible bases, either

$$(56)\quad \mathrm{m-scheme}\quad |\Phi_\alpha\rangle = \Pi_{nljm\tau} a_i^+|0\rangle = a_{i1}^+ \cdots a_{iA}^+|0\rangle \ , D \sim \begin{pmatrix} d_\pi \\ p \end{pmatrix} \cdot \begin{pmatrix} d_\nu \\ n \end{pmatrix} \ ,$$

which is simple, based on the Slater determinants, and the corresponding hamiltonian matrix is sparse, but it has a huge dimension (d_π, d_ν are the dimensions of the proton and neutron included subshells and p, n are the numbers of valence protons and neutrons). The other possible basis uses states coupled to a given total angular momentum J and isospin T. The dimensions are smaller in that case but the evaluation of the hamiltonian matrix element is more complicated and the corresponding hamiltonian matrix has fewer zero entries. Due to the high dimensionality of the problem one cannot include in the valence space too many single-particle orbits. Even the most advanced evaluations include just one oscillator shell, in most $\beta\beta$ decay candidate nuclei the valence space usually omits important spin-orbit partners. (For ^{76}Ge for example, the valence space consists of $p_{1/2}, p_{3/2}, f_{5/2}$ and $g_{9/2}$ orbits for protons and neutrons, while omitting the essentially occupied $f_{7/2}$ and empty $g_{7/2}$ spin-orbit partners.)

Nucleus	^{128}Sn	^{130}Sn	^{132}Sb	^{132}Te	^{133}Te
Transition	$0^+ \to 1^+$	$0^+ \to 1^+$	$4^+ \to 3,4,5^+$	$0^+ \to 1^+$	$\frac{3}{2}^+ \to \frac{1}{2}, \frac{3}{2}, \frac{5}{2}^+$
$T_{1/2}$exp.	59.07m	3.72m	2.79m	3.2d	12.5m
$T_{1/2}$calc. (0.74)	32.21m	2.47m	1.56m	1.73d	6.42m
Renorm.	0.54	0.6	0.55	0.54	0.53

^{134}Te	^{135}Xe	^{136}Cs
$0^+ \to 1^+$	$\frac{3}{2}^+ \to \frac{1}{2}, \frac{3}{2}, \frac{5}{2}^+$	$5^+ \to 4,5,6^+$
41.8m	9.14h	13.16d
29.19m	7.07h	8.1d
0.62	0.63	0.57

Fig. 14. – Experimental and calculated β-decay half-lives for several nuclei with A = 128-136 (adopted from ref. [56]).

In order to evaluate $M^{0\nu}$ the closure approximation is used and thus one evaluates

$$\langle f||O^K||i\rangle > \quad \text{with} \quad O^K = \Sigma_{ijkl} W^{\lambda,K}_{ijkl} \left[(a_i^+ a_j^+)^\lambda (\tilde{a}_k \tilde{a}_l)^\lambda\right]^0 \ , \tag{57}$$

where the creation operators create two protons and the annihilation operators annihilate two neutrons. In this way the problem is reduced to a standard nuclear structure problem where the many-body problem is reduced to the of evaluation of two-body transition densities. The matrix elements $W^{\lambda,K}_{ijkl}$ involve only the mean field (usually harmonic oscillator) one-body wave functions, and the transition operator defined above.

The hamiltonian H_{eff} is an effective operator. It is not entirely based on first principle reduction of the free nucleon-nucleon potential. Instead it relies on empirical data, in particular on the energies of states in semi-magic nuclei. At the same time effective operators should be used, in principle. Again, there is no well defined and well tested procedure to obtain their form. Instead, one uses empirical data and effective couplings (effective charges for the electromagnetic transitions, effective g_A values for the weak transitions).

How this procedure works is illustrated in Fig. 14 where the experimental β decay half-lives for a number of nuclei are compared with calculation and a quenching factor, i.e. the reduction factor of g_A^2 of $\sim$0.57 is obtained. And in Fig. 15 we show the same comparison for the evaluation of the $2\nu\beta\beta$ half-lives. (Note that this table is a bit obsolete as far as the experimental data are concerned. In the meantime, the $T_{1/2}$ for ^{130}Te was directly determined as 7.6×10^{20} years, and the limit for $T_{1/2}$ in ^{136}Xe is longer than indicated, $T_{1/2} > 1.0 \times 10^{22}$ years, see the Table in the preceding section.)

Various aspects of the application of the NSM to the $\beta\beta$ decay were reported in a number of publications [57, 58, 59, 60, 61, 62, 63]. We will return to these results later when we compare the NSM and QRPA methods.

Parent nuclei	^{48}Ca	^{76}Ge	^{82}Se	^{130}Te	^{136}Xe
$T^{2\nu}_{1/2}(g.s.)$ th.	$3.7E19$	$1.15E21$	$3.4E19$	$4E20$	$6E20$
$T^{2\nu}_{1/2}(g.s.)$ exp	$4.2E19$	$1.4E21$	$8.3E19$	$2.7E21$	$> 8.1E20$

Fig. 15. – Experimental and calculated $2\nu\beta\beta$-decay half-lives for several nuclei (adopted from ref. [56]).

Here we wish to stress one general result of NSM evaluation of $M^{0\nu}$. In the NSM one can classify states by their "seniority", i.e. by the number of valence nucleons that do not form Cooper-like pair and are therefore not coupled to $I^\pi = 0^+$. The dimensionality of the problem increases fast with seniority and thus it is of interest to see whether a truncation in seniority is possible and in general how the magnitude of $M^{0\nu}$ behaves as a function of the included seniority. This is illustrated in Fig. 16 from Ref. [63] for the case of the ^{76}Ge decay. Note that the result does not saturate until $s_m = 12$ which is nearly the maximum seniority possible. That behavior is observed in other cases as well (the saturation in s_m is faster in cases when one of the involved nuclei is semimagic) , and is relevant when the comparison to QRPA is made.

NSM can also successfully describe nuclear deformation, unlike the usual application of QRPA. Many of the considered $\beta\beta$ decay candidate nuclei are spherical or nearly so. However, one seemingly attractive candidate nucleus, ^{150}Nd, is strongly deformed. Moreover, the final nucleus, ^{150}Sm, is considerably less deformed than ^{150}Nd. Unfortunately, the NSM is unable to describe this system, the dimension is just too large. However, to see qualitatively what the effect of deformation is, or the difference in deformation,

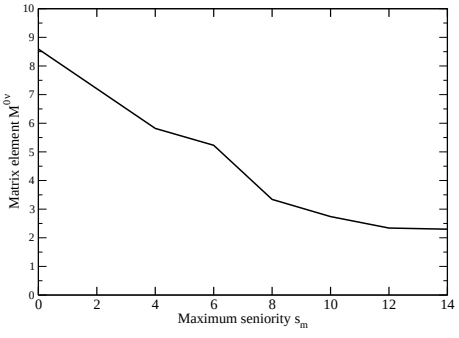

Fig. 16. – The full matrix element $M^{0\nu}$ for the ^{76}Ge $\rightarrow^{76}$Se transition evaluated with the indicated maximum seniority s_m included (adopted from ref. [63]).

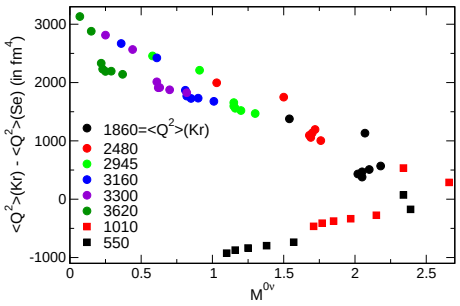

Fig. 17. – The matrix element $M^{0\nu}$ for the ^{82}Se $\rightarrow ^{82}$Kr transition for a large number of added quadrupole-quadrupole interaction strengths that induces increased deformation in ^{82}Se. The magnitude of $M^{0\nu}$ is ploted against the difference in the squared quadrupole moments of the invloved nuclei. (adopted from ref. [63]).

might be, in Ref. [63] the transition ^{82}Se $\rightarrow ^{82}$Kr was considered and the initial nucleus ^{82}Se was artificially deformed by including in the hamiltonian an additional (unrealistic) quadrupole-quadrupole interaction of varying strength. The result of that exercise are shown in Fig. 17. One can see that as the difference in deformation increases that magnitude of $M^{0\nu}$ decreases considerably.

What are, then, the outstanding issues for NSM vis-a-vis the evaluation of the $M^{0\nu}$ matrix elements? The most important one, in my opinion, is the limited size of the valence space. It is not clear how large (or small) the effect of the additional orbits might be. They cannot be, at present, included directly. Perhaps a perturbative method of including them can be developed, either in the shell model codes or in the definition of the effective operator. The other issue, that perhaps could be overcome, is the fact that the H_{eff} has not been determined for nuclei with $A = 90 - 110$ and thus the $M^{0\nu}$ are not available. Among them are important $\beta\beta$ candidate nuclei ^{100}Mo and ^{96}Zr (a definitive calculations for ^{116}Cd were not reported as yet either).

6˙2. *QRPA basics*. – The QRPA method was first applied to the charge changing modes by Halbleib and Sorensen [64] long time ago and generalized to include the particle-particle interaction by Cha [65]. The use of quasiparticles in QRPA makes it possible to include the pairing correlations in the nuclear ground states in a simple fashion. With pairing included, the Fermi levels for protons and neutrons not only become diffuse, but the number of nucleons in each subshell will not have a sharp value, instead only a mean occupancy of each subshell will have a well determined value.

To include the pairing we perform first the Bogoliubov transformation relating the particle creation and annihilation operators $a^{\dagger}_{jm}, \tilde{a}_{jm}$ with the quasiparticle creation and

annihilation operators $c^\dagger_{jm}, \tilde{c}_{jm}$,

$$\begin{pmatrix} a^\dagger_{jm} \\ \tilde{a}_{jm} \end{pmatrix} = \begin{pmatrix} u_j c^\dagger_{jm} & + & v_j \tilde{c}_{jm} \\ -v_j c^\dagger_{jm} & + & u_j \tilde{c}_{jm} \end{pmatrix} , \tag{58}$$

where $\tilde{a}_{jm} = (-1)^{j-m} a_{j-m}$ and $u_j^2 + v_j^2 = 1$.

The amplitudes u_j, v_j are determined in the standard way by solving the BCS gap equations, separately for protons and neutrons,

$$\Delta_a = (2j_a+1)^{-1/2} \Sigma_c (2j_c+1)^{1/2} u_c v_c \langle j_a^2; 0^+ || V || j_c^2; 0^+ \rangle \ , \qquad N = \Sigma_c (2j_c+1) v_c^2 \ . \tag{59}$$

Here N is the number of neutrons or protons and the gaps Δ are empirical quantities deduced from the usual mass differences of the corresponding even-even and odd-A nuclei. We renormalize the strength of the pairing interaction (the coupling constant in $\langle j_a^2; 0^+ || V || j_c^2; 0^+ \rangle$) slightly such that the empirical gaps Δ are correctly reproduced.

Our goal is to evaluate the transition amplitudes associated with charge changing one-body operator T^{JM} connecting the 0^+ BCS vacuum $|O\rangle$ of the quasiparticles c and $c^\dagger$ in the even-even nucleus with any of the J^π excited states in the neighboring odd-odd nuclei. In the spirit of RPA we describe such states as harmonic oscillations above the BCS vacuum. Thus

$$|J^\pi M; m\rangle = \Sigma_{pn} \left[X^m_{pn,J\pi} A^\dagger(pn; J^\pi M) + Y^m_{pn,J\pi} \tilde{A}(pn; J^\pi M) \right] |0^+_{QRPA}\rangle \ , \tag{60}$$

where

$$\begin{aligned} A^\dagger(pn; J^\pi M) &= \Sigma_{m_p, m_n} \langle j_p m_p, j_n m_n | JM \rangle c^\dagger_{j_p, m_p} c^\dagger_{j_n m_n} \\ \tilde{A}(pn; J^\pi M) &= (-1)^{J-M} A(pn; J^\pi - M) \ , \end{aligned} \tag{61}$$

and $0^+_{QRPA}\rangle$ is the "phonon vacuum" a correlated state that has the zero-point motion corresponding to the given J^π built into it. It contains, in addition to the BCS vacuum, components with 4, 8, etc. quasiparticles.

The so-called forward- and backward-going amplitudes X and Y as well as the corresponding energy eigenvalues ω_m are determined by solving the QRPA eigenvalue equations for each J^π

$$\begin{pmatrix} A & B \\ -B & -A \end{pmatrix} \begin{pmatrix} X \\ Y \end{pmatrix} = \omega \begin{pmatrix} X \\ Y \end{pmatrix} \ . \tag{62}$$

It is easy to see that eq. (62) is, in fact, an eigenvalue equation for ω^2 of the type $(A^2 - B^2)X = \omega^2 X$. Hence the physical solutions are such that ω^2 is positive, and we can choose ω to be positive as well. On the other hand, there could be unphysical solutions with $\omega^2 < 0$ and hence imaginary energies. By varying the coupling constants in the matrices A and B we might trace the development of the solutions from the physical ones

with $\omega > 0$ to the situation where $\omega = 0$. That point signals the onset of region where the original RPA (or QRPA) is no longer applicable, because the ground state must be rearranged. Examples are the transition from a spherical to deform shape, or transition from pairing of neutrons with neutrons (and protons with protons) to a pairing involving neutron-proton pairs. We will see that real nuclei are rather close to that latter situation, and we need to worry about the applicability of the method in such situations.

To obtain the matrices A and B one needs first to rewrite the hamiltonian in the quasiparticle representation. Then

$$\begin{aligned} A^J_{pn,p'n'} &= \langle O|(c^\dagger_p c^\dagger_n)^{(JM)^\dagger}\hat{H}(c^\dagger_{p'}c^\dagger_{n'})^{(JM)}|O\rangle \\ &= \delta_{pn,p'n'}(E_p + E_n) \\ &\quad +(u_p v_n u_{p'} v_{n'} + v_p u_n v_{p'} u_{n'})g_{ph}\langle pn^{-1}, J|V|p'n'^{-1}, J\rangle \\ &\quad +(u_p u_n u_{p'} u_{n'} + v_p v_n v_{p'} v_{n'})g_{pp}\langle pn, J|V|p'n', J\rangle \ , \end{aligned} \tag{63}$$

and

$$\begin{aligned} B^J_{pn,p'n'} &= \langle O|\hat{H}(c^\dagger_p c^\dagger_n)^{(J-M)}(-1)^M(c^\dagger_{p'}c^\dagger_{n'})^{(JM)}|O\rangle \\ &\quad +(-1)^J(u_p v_n v_{p'} u_{n'} + v_p u_n u_{p'} v_{n'})g_{ph}\langle pn^{-1}, J|V|p'n'^{-1}, J\rangle \\ &\quad -(-1)^J(u_p u_n v_{p'} v_{n'} + v_p v_n u_{p'} u_{n'})g_{pp}\langle pn, J|V|p'n', J\rangle \ . \end{aligned} \tag{64}$$

Here E_p, E_n are the quasiparticle energies. The particle-hole and particle-particle interaction matrix elements are related to each other by the Pandya trasformation

$$\langle pn^{-1}, J|V|p'n'^{-1}, J\rangle = -\Sigma_{J'}(2J'+1)\left\{ \begin{array}{ccc} p & n & J \\ p' & n' & J' \end{array} \right\}\langle pn', J|V|p'n, J\rangle \tag{65}$$

Above, in eqs. (64, 65) we have introduced adjustable renormalization constants g_{ph} and g_{pp} that multiply the whole block of interaction matrix elements for particle-hole and particle-particle configurations. Typically, one uses a realistic interaction for V (G-matrix) and thus the nominal values are $g_{ph} = g_{pp} = 1$.

The vectors X and Y obey the normalization and orthogonality conditions (for each J^π)

$$\begin{aligned} \Sigma_{pn} X^m_{pn}X^{m'}_{pn} - Y^m_{pn}Y^{m'}_{pn} &= \delta_{m,m'} \\ \Sigma_m X^m_{pn}X^m_{p'n'} - Y^m_{pn}Y^m_{p'n'} &= \delta_{pn,p'n'} \\ \Sigma_{pn} X^m_{pn}Y^{m'}_{pn} - Y^m_{pn}X^{m'}_{pn} &= 0 \\ \Sigma_m X^m_{pn}Y^m_{p'n'} - Y^m_{pn}X^m_{p'n'} &= 0 \end{aligned} \tag{66}$$

For a one-body charge-changing operator T^{JM} the transition amplitude connecting the ground state of an even-even (N, Z) nucleus to the mth excited state in the odd-odd

$(N-1, Z+1)$ nucleus is

$$\langle m; JM|T^{JM}|0^+_{QRPA}\rangle = \Sigma_{pn}\left[t^-_{pn}X^m_{pn,J\pi} + t^+_{pn}Y^m_{pn,J\pi}\right] \ , \tag{67}$$

where

$$t^-_{pn} = \frac{u_p v_n}{\sqrt{(2J+1)}}\langle p||T^J||n\rangle \ , \quad t^+_{pn} = (-1)^J\frac{v_p u_n}{\sqrt{(2J+1)}}\langle p||T^J||n\rangle \ . \tag{68}$$

The transition in the opposite direction, to the $(N+1, Z-1)$ is governed by analogous formula but with X and Y interchanged.

Given these formulae, we are able to calculate, within QRPA, the $\beta\beta$ decay nuclear matrix elements, for both 2ν and 0ν modes. However, one needs to make another approximation, since the initial state $|0^+_{QRPA}; i\rangle$ and the final state $|0^+_{QRPA}; f\rangle$ are not identical. This is a "two vacua" problem. The standard way of accounting for the difference in the initial and final states is to add the overlap factor

$$\langle J^\pi_k|J^\pi_m\rangle = \Sigma_{pn}X^k_{pn}\tilde{X}^m_{pn} - Y^k_{pn}\tilde{Y}^m_{pn} \ , \tag{69}$$

where $\tilde{X}, \tilde{Y}$ are the solutions of the QRPA equations of motion for the final nucleus.

We can now write down the formula for the $2\nu\beta\beta$-decay matrix element as

$$\begin{aligned} M^{2\nu} &= \Sigma_{k,m}\frac{\langle f||\vec{\sigma}\tau^+||1^+_k\rangle\langle 1^+_k|1^+_m\rangle\langle 1^+_m||\vec{\sigma}\tau^+||i\rangle}{\omega_m - (M_i+M_f)/2} \ , \\ \langle 1^+_m||\vec{\sigma}\tau^+||i\rangle &= \Sigma_{pn}\langle p||\vec{\sigma}||n\rangle(u_p v_n X^m_{pn} + v_p u_n Y^m_{pn}) \\ \langle f||\vec{\sigma}\tau^+||1^+_k\rangle &= \Sigma_{pn}\langle p||\vec{\sigma}||n\rangle(\tilde{v}_p\tilde{u}_n\tilde{X}^k_{pn} + \tilde{u}_p\tilde{v}_n\tilde{Y}^k_{pn}) \ . \end{aligned} \tag{70}$$

For the 0ν decay the corresponding formula is

$$\begin{aligned} M_K = &\sum_{J^\pi,k_i,k_f,\mathcal{J}}\sum_{pnp'n'}(-1)^{j_n+j_{p'}+J+\mathcal{J}}\times \\ &\sqrt{2\mathcal{J}+1}\left\{\begin{array}{ccc} j_p & j_n & J \\ j_{n'} & j_{p'} & \mathcal{J}\end{array}\right\}\times \\ &\langle p(1), p'(2); \mathcal{J} \parallel \bar{f}(r_{12})\tau^+_1\tau^+_2 O_K \bar{f}(r_{12}) \parallel n(1), n'(2); \mathcal{J}\rangle \times \\ &\langle 0^+_f|||\widetilde{[c^+_{p'}\tilde{c}_{n'}]_J}||J^\pi k_f\rangle\langle J^\pi k_f|J^\pi k_i\rangle\langle J^\pi k_f i|||[c^+_p\tilde{c}_n]_J||0^+_i\rangle \ . \end{aligned} \tag{71}$$

The operators $O_K, K =$ Fermi (F), Gamow-Teller (GT), and Tensor (T) contain neutrino potentials, see eq. (54), and spin and isospin operators, and RPA energies $E^{k_i,k_f}_{J^\pi}$. The reduced matrix elements of the one-body operators $[c^+_p\tilde{c}_n]_J$ in eq. (71) depend on the BCS coefficients u_i, v_j and on the QRPA vectors X, Y; they are just the reduced matrix elements of the one-body operators like in eqs. (67, 68). The function $\bar{f}(r_{12})$ in above represents the effect of short range correlations. These will be discussed in detail in the next Section. Note, that the radial matrix elements in eq. (71) are evaluated with

unsymmetrized two-particle wave functions. This is a generic requirement of RPA-like procedures as explained in Ref.[66]

6˙3. *Generalization - RQRPA.* – The crucial simplifying point of QRPA (or RPA-like procedures in general) is the quasiboson approximation, the assumption that the commutation relations of a pair of fermion operators can be replaced by the boson commutation relation. That is a good approximation for harmonic, small amplitude excitations. However, when the strength of the attractive particle-particle interaction increases, the number of quasiparticles in the correlated ground state $|0^+_{QRPA}\rangle$ increases and thus the method violates the Pauli principle. This, in turn, leads to an overestimate of ground state correlations, and too early onset of the QRPA collapse.

To cure this problem, to some extent, a simple procedure, so-called renormalized QRPA (RQRPA) has been proposed and is widely used [67]. In RQRPA the exact expectation value of a commutator of two-bifermion operators is replaced by

$$\langle 0^+_{QRPA}|\big[A(pn,JM),A^+(p'n',JM)\big]|0^+_{QRPA}\rangle = \delta_{pp'}\delta_{nn'}\times \underbrace{\Big\{1-\frac{1}{\hat{j}_l}<0^+_{QRPA}|[a^+_p\tilde{a}_p]_{00}|0^+_{QRPA}>-\frac{1}{\hat{j}_k}<0^+_{QRPA}|[a^+_n\tilde{a}_n]_{00}|0^+_{QRPA}>\Big\}}_{\mathcal{D}_{pn,J^\pi}}, \tag{72}$$

with $\hat{j}_p=\sqrt{2j_p+1}$.

To take this generalization into account, i.e. the nonvanishing values of $\mathcal{D}_{pn,J^\pi}-1$ one simply needs to use the amplitudes

$$\overline{X}^m_{(pn,J^\pi)}=\mathcal{D}^{1/2}_{pn,J^\pi}\ X^m_{(pn,J^\pi)},\qquad \overline{Y}^m_{(pn,J^\pi)}=\mathcal{D}^{1/2}_{pn,J^\pi}\ Y^m_{(pn,J^\pi)}\ , \tag{73}$$

which are orthonormalized in the usual way instead of the standard X and Y everywhere also in the QRPA equation of motion (62). In addition, the matrix elements of the one-body operators, eqs. (67, 68), must be multiplied by $\mathcal{D}^{1/2}_{pn,J^\pi}$ evaluated for the initial and final nuclei.

In order to calculate the factors $\mathcal{D}^{1/2}_{pn,J^\pi}$ one has to use an iterative procedure and evaluate in each iteration

$$\begin{aligned} D_{pn}=1&-\frac{1}{2j_p+1}\Sigma_{n'}D_{pn'}\left(\Sigma_{J,k}(2J+1)|\overline{Y}^{J,k}_{pn'}|^2\right)\\ &-\frac{1}{2j_n+1}\Sigma_{p'}D_{p'n}\left(\Sigma_{J,k}(2J+1)|\overline{Y}^{J,k}_{p'n}|^2\right)\ . \end{aligned} \tag{74}$$

Note the summation over the multipolarity J. Even if for the 2ν decay only $J^\pi=1^+$ are seemingly needed, in RQRPA the equations need to be solved for all multipoles.

7. – Numerical calculations in QRPA and RQRPA

In the previous section all relevant expressions were given. But that is not all one needs in order to evaluate the nuclear matrix elements numerically. One has to decide, first of all, what are the relevant input parameters, and how to choose them.

The first one to choose, as in all nuclear structure calculations, is the mean field potential, and which orbits are going to be included in the corresponding expressions. A typical choice is the calculation based on the Coulomb corrected Woods-Saxon potential. However, sometimes it is advisable to modify the single particle energy levels in order to better describe certain experimental data (energies in the odd-A nuclei or occupation numbers).

Next one needs to choose the nucleon-nucleon potential. For that one typically uses a G-matrix based on a realistic force. For example, in [66] the G-matrix used was derived from the Bonn-CD nucleon-nucleon force. It turns out that the results only weakly depend on which parametrization of the nucleon-nucleon interaction is used.

Next, the effective coupling constants g_{ph} and g_{pp} in the matrices A and B in equation of motion (62) must be determined. The parameter g_{ph} is not controversial. It is usually adjusted by requiring that the energy of some chosen collective states, often Gamow-Teller (GT) giant resonances, is correctly reproduced. It turns out that the calculated energy of the giant GT state is almost independent of the size of the single-particle basis and is well reproduced with $g_{ph} \approx 1$. Hence, the nominal and unrenormalized value $g_{ph} = 1$ is used in most calculations; that reduces the number of adjustable parameters as well.

The choice of the particle-particle parameter g_{pp} is, however, not only important, but also to some extent controversial. One of the issues involved is illustrated in Fig. 18. There, one can see that the curves of $M^{2\nu}$ versus g_{pp} are rather different for different number of included single-paricle states. Thus, the calculated magnitude of $M^{2\nu}$ will change dramatically if g_{pp} is fixed and different number of levels is included.

The other feature, illustrated in Fig. 18 is the crossing of $M^{2\nu}$ of zero value for certain g_{pp} that is relatively close to unity. This was first recognized long time ago in Ref. [69]. Obviously, if $M^{2\nu} = 0$ then the $2\nu\beta\beta$-decay lifetime is infinite, this is a absolute suppression of that mode. Past that zero crossing the curves become very steep and the collapse of QRPA is reached when the slope becomes vertical. Obviously, the zero crossing is moved to larger values of g_{pp} in RQRPA.

One can use all of this to an advantage by abandoning the goal of predicting the $M^{2\nu}$ values, but instead of using the experimental $M^{2\nu}$ and determine the g_{pp} (for a given set of s.p. states) in such a way, that the correct $M^{2\nu}$ is obtained. That is illustrated in Fig. 19. The resulting g_{pp} then depends on the number of included single-particle states, and is typically in the range $0.8 \leq g_{pp} \leq 1.2$ when a realistic G-matrix based hamiltonian is used.

Adjusting the value of g_{pp} such that the $M^{2\nu}$ is correctly reproduced has been criticized, e.g. in Ref. [70]. There an alternative method, based on the experimentally known β-decay ft values connecting the ground state of the intermediate nucleus (if that hap-

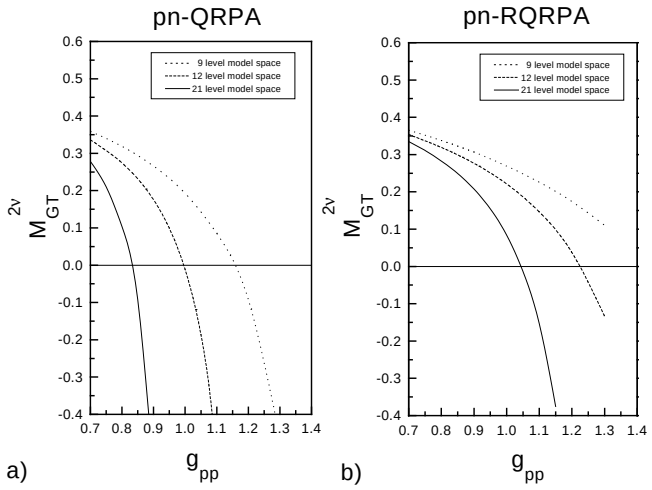

Fig. 18. – The matrix elements $M^{2\nu}$ for ^{76}Ge evaluated in QRPA (panel a) and RQRPA (panel b). The calculation was performed with the indicated number of included single-particle states. (Adopted from [68]). The experimental value of $M^{2\nu}$ is 0.13 MeV^{-1}.

pens to be 1^+, which is so only in ^{100}Tc, ^{116}In and ^{128}I among the $\beta\beta$-decay candidates). In QRPA the transition amplitudes for the EC process (decreasing nuclear charge) and β^- (increasing nuclear charge) move in opposite way when g_{pp} is increased; the first one goes up while the second one goes down. It is difficult, and essentially impossible to describe all three experimental quantities with the same value of g_{pp} (in the case of ^{100}Mo this was noted already in [71]).

While the differences between these two approaches are not very large (see [72]), there

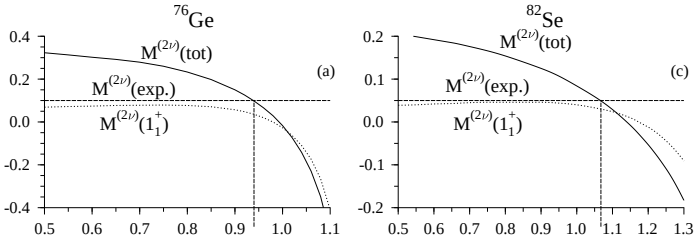

Fig. 19. – The calculated 2ν matrix elements for ^{76}Ge and ^{82}Se as a function of g_{pp} (solid lines). The experimental values are indicated by the horizontal dashed lines. The dotted line indicates the contribution of the first 1^+ state. (Adopted from[70].)

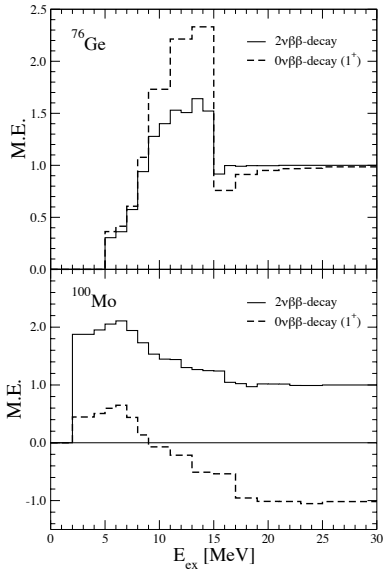

Fig. 20. – Running sum of the $2\nu\beta\beta$-decay and $0\nu\beta\beta$-decay (only 1^+ component) matrix elements for ^{76}Ge and ^{100}Mo (normalized to unity) as a function of the excitation energy $E_{ex} = E_n - (E_i + E_f)/2$.

are other arguments why choosing the agreement with $M^{2\nu}$ is preferable. First, it is not really true that the first 1^+ state is the only one responsible for the $2\nu\beta\beta$ decay. This is illustrated for the cases of ^{76}Ge and ^{100}Mo in Fig. 20. Even though for ^{100}Mo the first state contributes substantially, higher lying states give non-negligible contribution. And in ^{76}Ge many 1^+ states give comparable contribution. Thus, to give preference to the lowest state is not well justified, the sum is actually what matters. At the same time, the dilemma that the β^- and β^+/EC matrix elements move with g_{pp} in opposite directions makes it difficult to choose one of them. It seems better to use the sum of the products of the amplitudes, i.e. the $2\nu\beta\beta$ decay.

At the same time, the contribution of the 1^+ multipole to the $0\nu\beta\beta$ matrix element and the corresponding $2\nu\beta\beta$ matrix element are correlated, even though they are not identical, as also shown in Fig. 20. Making sure that the $2\nu\beta\beta$ matrix element agrees with its experimental value constrains the 1^+ part of the $0\nu\beta\beta$ matrix element as well.

Since we are really interested in the $M^{0\nu}$ matrix element, it is relevant to ask why do we fit the important parameter g_{pp} to the 2ν decay lifetime. To understand this, it is useful to point out that two separate multipole decompositions are built into Eq. (71). One is in terms the J^π of the virtual states in the intermediate nucleus, the good quantum numbers of the QRPA and RQRPA. The other decomposition is based on the angular momenta and parities $\mathcal{J}^\pi$ of the pairs of neutrons that are transformed into protons with the same $\mathcal{J}^\pi$.

In Fig. 21 we show that it is essentially only the 1^+ multipole that is responsible for

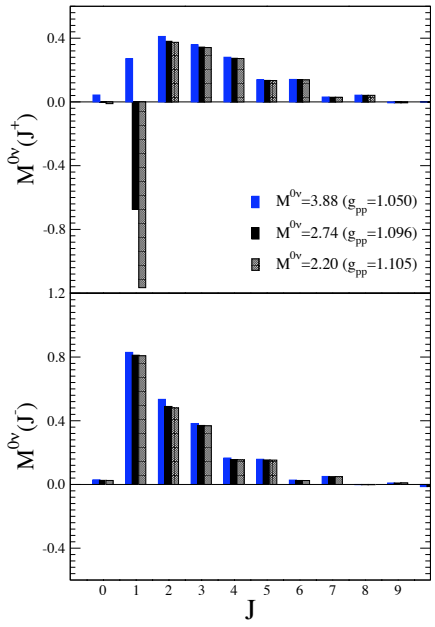

Fig. 21. – The contributions of different intermediate-state angular momenta J^π to $M^{0\nu}$ in ^{100}Mo (positive parities in the upper panel and negative parities in the lower one). We show the results for several values of g_{pp}. The contribution of the 1^+ multipole changes rapidly with g_{pp}, while those of the other multipoles change slowly.

the variation of $M^{0\nu}$ with g_{pp}. (Note that in the three variants shown the parameter g_{pp} changes only by 5%.) Fixing its contribution to a related observable (2ν decay) involving the same initial and final nuclear states appears to be an optimal procedure for determining g_{pp}. Moreover, as was shown in [73, 72], this choice, in addition, essentially removes the dependence of $M^{0\nu}$ on the number of the single-particle states (or oscillator shells) in the calculations.

7˙1. *Competition between 'pairing' and 'broken pairs'.* – The decomposition based on the angular momenta and parities $\mathcal{J}^\pi$ of the pairs of neutrons that are transformed into protons with the same $\mathcal{J}^\pi$ is particularly revealing. In Fig. 22 we illustrate it both in the NSM and QRPA, with the same single-single particle spaces in each. These two rather different approaches agree in a semiquantitative way, but the NSM entries for $\mathcal{J} > 0$ are systematically smaller in absolute value. There are two opposing tendencies in Fig. 22. The large positive contribution (essentialy the same in QRPA and NSM) is associated with the so-called pairing interaction of neutrons with neutrons and protons with protons. As the result of that interaction the nuclear ground state is mainly composed of Cooper-like pairs of neutrons and protons coupled to $\mathcal{J} = 0$. The transformation of one neutron

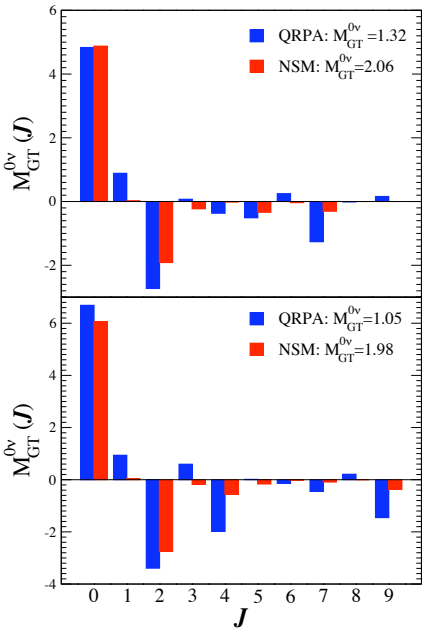

Fig. 22. – Contributions of different angular momenta $\mathcal{J}$ associated with the two decaying neutrons to the Gamow-Teller part of $M^{0\nu}$ in ^{82}Se (upper panel) and ^{130}Te (lower panel). The results of NSM (dark histogram) and QRPA treatments (lighter histogram) are compared. Both calculations use the same single-particle spaces: $(f_{5/2}, p_{3/2}, p_{1/2}, g_{9/2})$ for ^{82}Se and $(g_{7/2}, d_{5/2}, d_{3/2}, s_{1/2}, h_{11/2})$ for ^{130}Te. In the QRPA calculation the particle-particle interaction was adjusted to reproduce the experimental $2\nu\beta\beta$-decay rate.

Cooper pair into one Cooper proton pair is responsible for the $\mathcal{J} = 0$ piece in Fig. 22.

However, the nuclear hamiltonian contains, in addition, important neutron-proton interaction. That interaction, primarily, causes presence in the nuclear ground state of "broken pairs", i.e. pairs of neutrons or protons coupled to $\mathcal{J} \neq 0$. Their effect, as seen in Fig. 22, is to reduce drastically the magnitude of $M^{0\nu}$. In treating these terms, the agreement between QRPA and NSM is only semi-quantitative. Since the pieces related to the "pairing" and "broken pairs" contribution ale almost of the same magnitude but of opposite signs, an error in one of these two competing tendencies is enhanced in the final $M^{0\nu}$. The competition, illustrated in Fig. 22, is the main reason behind the spread of the published $M^{0\nu}$ calculations. Many authors use different, and sometimes inconsistent, treatment of the neutron-proton interaction.

There are many evaluations of the matrix elements $M^{0\nu}$ in the literature (for the latest review see [21]). However, the resulting matrix elements often do not agree with each other as mentioned above and it is difficult, based on the published material, to decide who is right and who is wrong, and what is the theoretical uncertainty in $M^{0\nu}$. That

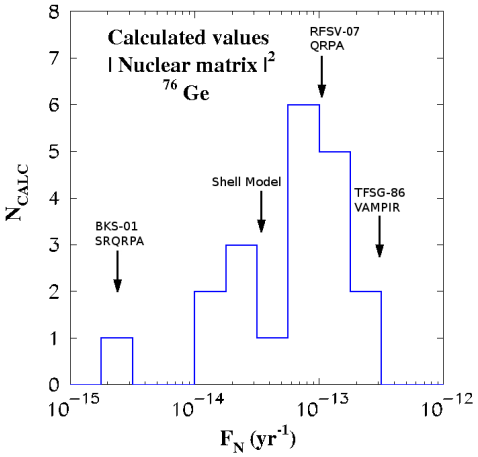

BKS-01 = A. Bobyk, W. Kaminski, F. Simkovic, PRC**63** (2001) ⇐ $2\nu\beta\beta$ 20 times too slow
Shell Model = E. Caurier, G. Martinez-Pinedo, F. Nowacki, A. Poves A. Zuker, RMP**77** (2005)
RFSV-07 = V.R., A. Faessler, F. Simkovic, P. Vogel, NPA**793** (2007) (2003) ⇐ $2\nu\beta\beta$ fitted
TFSG-86 = T. Tomoda, A. Faessler, K. W. Schmid, F. Grummer, NPA**452** (1986)
⇐ $2\nu\beta\beta$ 8 times too fast

Fig. 23. – Histogram of older published calculated values of $(M^{0\nu})^2$ for ^{76}Ge. The failure of some of the calculations to reproduce the known $2\nu\beta\beta$-decay lifetime is indicated.

was stressed in a powerful way in the paper by Bahcall *et al.* few years ago [74] where a histogram of 20 calculated values of $(M^{0\nu})^2$ for ^{76}Ge was plotted, with the implication that the width of that histogram is a measure of uncertainty. That is clearly not a valid conclusion as one could see in Fig. 23 where the failure of the outliers to reproduce the known $2\nu\beta\beta$-decay lifetime is indicated.

To see some additional reasons why different authors obtain in their calculations different nuclear matrix elements we need to analyze the dependence of the $M^{0\nu}$ on the distance r between the pair of initial neutrons (and, naturally, the pair of final protons) that are transformed in the decay process. That analysis reveals, at the same time, the various physics ingredients that must be included in the calculations so that realistic values of the $M^{0\nu}$ can be obtained.

7˙2. *Dependence on the radial distance.* – The simplest and most important neutrino potential has the form (already defined in eq. (41))

$$H(r) \sim \frac{R}{r}\Phi(\omega r) \ , \tag{75}$$

where R is the nuclear radius introduced here as usual to make the potential, and the resulting $M^{0\nu}$, dimensionless (the $1/R^2$ in the phase space factor compensates for this),

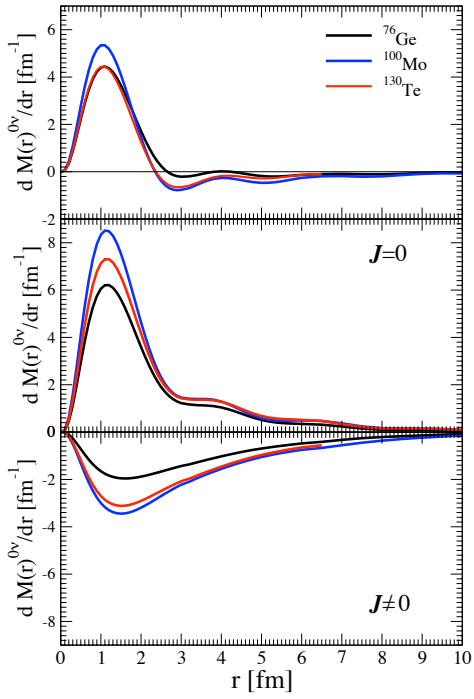

Fig. 24. – The dependence on r of $M^{0\nu}$ for ^{76}Ge, ^{100}Mo and ^{130}Te. The upper panel shows the full matrix element, and the lower panel shows separately 'pairing' ($\mathcal{J} = 0$ of the two participating neutrons) and 'broken pair' ($\mathcal{J} \neq 0$) contributions.

r is the distance between the transformed neutrons (or protons) and $\Phi(\omega r)$ is a rather slowly varying function of its argument.

From the form of the potential $H(r)$ one would, naively, expect that the characteristic value of r is the typical distance between the nucleons in a nucleus, namely that $\bar{r} \sim R$. However, that is not true as was demonstrated first in Ref. [66] and illustrated in Fig. 24. One can see there that the competition between the "pairing" and "broken pairs" pieces essentially removes all effects of $r \geq 2 - 3$ fm. Only the relatively short distances contribute significantly; essentially only the nearest neighbor neutrons undergo the $o\nu\beta\beta$ transition. The same result was obtained in the NSM [63]. (We have also shown in [66] that an analogous result is obtained in an exactly solvable, semirealistic model. There we also showed that this behaviour is restricted to an interval of the parameter g_{pp} that contains the realistic value near unity.)

Once the r dependence displayed in Fig. 24 is accepted, several new physics effects clearly need to be considered. These are not nuclear structure issue per se, since they are related more to the structure of the nucleon.

One of them is the short-range nucleon-nucleon repulsion known from scattering ex-

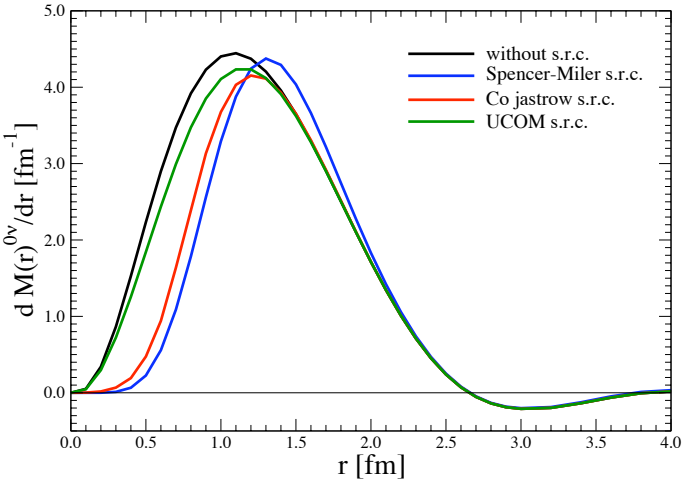

Fig. 25. – The r dependence of $M^{0\nu}$ in ^{76}Ge. The four curves show the effects of different treatments of short-range correlations. The resulting $M^{0\nu}$ values are 5.32 when the effect is ignored, 5.01 when the UCOM transformation is applied and 4.14 when the treatment based on the Fermi hypernetted chain and 3.98 when the phenomenological Jastrow function is used. (See the text for details.)

periments. Two nucleon strongly repel each other at distances $r \leq 0.5 - 1.0$ fm, i.e. the distances very relevant to evaluation of the $M^{0\nu}$. The nuclear wave functions used in QRPA and NSM, products of the mean field single-nucleon wave function, do not take into account the influence of this repulsion that is irrelevant in most standard nuclear structure theory applications. The usual and simplest way to include the effect is to modify the radial dependence of the $0\nu\beta\beta$ operator so that the effect of short distances (small values of r) is reduced. This is achieved by introducing a phenomenological function $\bar{f}(r_{12}$ in the eq. (71). Examples of such Jastrow-like function were first derived in [75] and in a more modern form in [76]. That phenomenological procedure reduces the magnitude of $M^{0\nu}$ by 20-25% as illustrated in Fig. 25. Recently, another procedure, based on the Unitary Correlation Operator Method (UCOM) has been proposed [77]. That procedure, still applied not fully consistently, reduces the $M^{0\nu}$ much less, only by about 5% [78]. It is prudent to include these two possibilities as extremes and the corresponding range as systematic error. Once a consistent procedure is developed, consisting of deriving an effective $0\nu\beta\beta$ decay operator that includes (probably perturbatively) the effect of the high momentum (or short range) that component of the systematic error could be substantially reduced.

Another effect that needs to be taken into account is the nucleon composite nature. At weak interaction reactions with higher momentum transfer the nucleon is less likely to remain nucleon; new particles for example pions, are often produced. That reduction is included, usually, by introducing the dipole form of the nucleon form factor, already

introduced,

$$f_{V,A} = \left(\frac{1}{1 + q^2/M_{V,A}^2} \right)^2 , \tag{76}$$

where the cut-off parameters $M_{V,A}$ have values (deduced in the reactions of free neutrinos with free or quasifree nucleons) ~ 1 GeV. This corresponds to the nuclon size of $\sim 0.5-1.0$ fm. Note that in our case we are dealing with neutrinos far off mass shell, and bound nucleons, hence it is not obvious that the above form factors are applicable. It turns out, however, that once the short range correlations are properly included (by either of the procedures discussed above) the $M^{0\nu}$ becomes essentially independent of the adopted values when $M_{V,A} \geq 1$ GeV. In the past various authors neglected the effect of short range correlations, and in that case a proper inclusion of nucleon form factor (or their neglect) again causes variations in the calculated $M^{0\nu}$ values.

Yet another correction that various authors neglected must be included in a correct treatment. Since $r \leq$ 2-3 fm is the relevant distances, the corresponding momentum transfer $1/r$ is of the order of $\sim$200 MeV, much larger than in the ordinary β decay. Hence the induced nucleon currents, in particular the pseudoscalar (since the neutrinos are far off mass shell) give noticeable contributions [66, 79].

Finally, the issue of the axial current "quenching" should be considered. As shown in a rather typical example in Fig. 14 calculated values of the GT β-decay matrix elements usually overestimate the corresponding experimental values. The reasons for that are, at least qualitatively understood, but the explanation is beyond the scope of these lectures. It suffice to say, that one can account for that effect phenomenologically and conveniently, by reducing the value of the axial-vector coupling constant g_A to ~ 1 instead of its true value 1.25. The phenomenon of quenching has been observed only in the GT β decays, so it is not clear whether the same reduction of g_A should be used also in the $0\nu\beta\beta$ decay. Nevertheless, it is prudent to include that possibility as a source of uncertainty. In anticipation , we already used the modified definition $M'^{0\nu}$, see eq. (55).

We have, therefore, identified the various physics effects that ought to be included in a realistic evaluation of $M^{0\nu}$ values. The spread of the calculated values, noted by Bahcall *et al.* [74] can be often attributed to the fact that various authors either neglect some of them, or include them inconsistently.

8. – Calculated $M'^{0\nu}$ values

Even though we were able to explain, or eliminate, a substantial part of the spread of the calculated values of the nuclear matrix elements, sizeable systematic uncertainty remains. That uncertainty, within QRPA and RQRPA, as discussed in Refs.[73, 72], is primarily related to the difference between these two procedures, to the size of the single-particle space included, whether the so-called quenching of the axial current coupling constant g_A is included or not, and to the systematic error in the treatment of short range correlations [66]. In Fig. 26 the full ranges of the resulting matrix elements $M^{0\nu}$

TABLE II. – *The calculated ranges of the nuclear matrix element $M^{'0\nu}$ evaluated within both the QRPA and RQRPA and with both standard ($g_A = 1.254$) and quenched ($g_A = 1.0$) axial-vector couplings. In each case we adjusted g_{pp} so that the rate of the $2\nu\beta\beta$=decay is reproduced. Column 2 contains the ranges of $M^{'0\nu}$ with the phenomenological Jastrow-type treatment of short range correlations (see I and II), while column 3 shows the UCOM-based results (see Ref. [77]). Columns 3 and 5 give the $0\nu\beta\beta$-decay half-life ranges corresponding to the matrix-element ranges in columns 2 and 4, for $< m_{\beta\beta} >= 50$ meV. Adapted from [66].*

Nuclear	(R)QRPA (Jastrow s.r.c.)		(R)QRPA (UCOM s.r.c.)	
transition	$M^{'0\nu}$	$T^{0\nu}_{1/2}$ ($\langle m_{\beta\beta}\rangle = 50$ meV)	$M^{'0\nu}$	$T^{0\nu}_{1/2}$ ($\langle m_{\beta\beta}\rangle = 50$ meV)
$^{76}Ge \rightarrow {}^{76}Se$	$(3.33, 4.68)$	$(6.01, 11.9) \times 10^{26}$	$(3.92, 5.73)$	$(4.01, 8.57) \times 10^{26}$
$^{82}Se \rightarrow {}^{82}Kr$	$(2.82, 4.17)$	$(1.71, 3.73) \times 10^{26}$	$(3.35, 5.09)$	$(1.14, 2.64) \times 10^{26}$
$^{96}Zr \rightarrow {}^{96}Mo$	$(1.01, 1.34)$	$(7.90, 13.9) \times 10^{26}$	$(1.31, 1.79)$	$(4.43, 8.27) \times 10^{26}$
$^{100}Mo \rightarrow {}^{100}Ru$	$(2.22, 3.53)$	$(1.46, 3.70) \times 10^{26}$	$(2.77, 4.58)$	$(8.69, 23.8) \times 10^{25}$
$^{116}Cd \rightarrow {}^{116}Sn$	$(1.83, 2.93)$	$(1.95, 5.01) \times 10^{26}$	$(2.18, 3.54)$	$(1.34, 3.53) \times 10^{26}$
$^{128}Te \rightarrow {}^{128}Xe$	$(2.46, 3.77)$	$(3.33, 7.81) \times 10^{27}$	$(3.06, 4.76)$	$(2.09, 5.05) \times 10^{27}$
$^{130}Te \rightarrow {}^{130}Xe$	$(2.27, 3.38)$	$(1.65, 3.66) \times 10^{26}$	$(2.84, 4.26)$	$(1.04, 2.34) \times 10^{26}$
$^{136}Xe \rightarrow {}^{136}Ba$	$(1.17, 2.22)$	$(3.59, 12.9) \times 10^{26}$	$(1.49, 2.76)$	$(2.32, 7.96) \times 10^{26}$

is indicated. The indicated error bars are highly correlated; e.g., if true values are near the lower end in one nucleus, they would be near the lower ends in all indicated nuclei.

The figure also shows the most recent NSM results [63]. Those results, obtained with Jastrow type short range correlation corrections, are noticeably lower than the QRPA values. That difference is particularly acute in the lighter nuclei ^{76}Ge and ^{82}Se. While the QRPA and NSM agree on many aspects of the problem, in particular on the role of the competition between "pairing" and "broken pairs" contributions and on the r dependence of the matrix elements, the disagreement in the actual values remains to be explained.

When one compares the 2ν and 0ν matrix elements (Figs. 10 and 26) the feature to notice is the fast variation in $M^{2\nu}$ when going from one nucleus to another while $M^{0\nu}$ change only rather smoothly, in both QRPA and NSM. This is presumably related to the high momentum transfer (or short range) involved in $0\nu\beta\beta$. That property of the $M^{0\nu}$ matrix elements makes the comparison of results obtained in different nuclei easier and more reliable.

Given the interest in the subject, we show the range of predicted half-lives corresponding to our full range of $M'^{0\nu}$ in Table II (for $\langle m_{\beta\beta}\rangle = 50$ meV). As we argued above, this is a rather conservative range within the QRPA and its related frameworks. One should keep in mind, however, the discrepancy between the QRPA and NSM results as well as systematic effects that might elude either or both calculations. Thus, as we

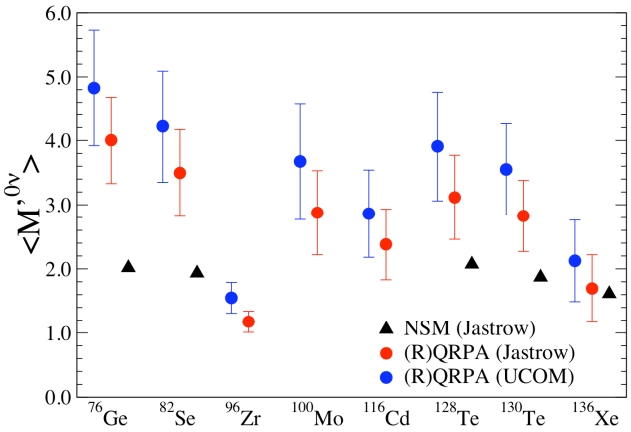

Fig. 26. – The full ranges of $M'^{0\nu}$ with the two alternative treatments of the short range correlations. For comparison the results of a recent Large Scale Shell Model evaluation of $M'^{0\nu}$ that used the Jastrow-type treatment of short range correlations are also shown (triangles).

have seen, while a substantial progress has been achieved, we are still somewhat far from being able to evaluate the $0\nu\beta\beta$ nuclear matrix elements confidently and accurately.

APPENDIX

Neutrino magnetic moment and the distinction between Dirac and Majorana neutrinos

The topic of neutrino magnetic moment μ_ν is seemingly unrelated to the $0\nu\beta\beta$ decay. Yet, as will be shown below, experimental observation of μ_ν allows one to make important conclusions about the Dirac versus Majorana nature of neutrinos. Hence, it is worthwhile to discuss it here.

Neutrino mass and magnetic moments are intimately related. In the orthodox Standard Model neutrinos have a vanishing mass and magnetic moments vanish as well. However, in the minimally extended SM containing gauge-singlet right-handed neutrinos the magnetic moment μ_ν is nonvanishing, but unobservably small [80],

$$\mu_\nu = \frac{3eG_F}{\sqrt{2}8\pi^2} m_\nu = 3 \times 10^{-19} \mu_B \frac{m_\nu}{1 \text{ eV}} \ . \tag{A.1}$$

An experimental observation of a magnetic moment larger than that given in eq.(A.1) would be an uneqivocal indication of physics beyond the minimally extended Standard Model.

Laboratory searches for neutrino magnetic moments are typically based on the obsevation of the $\nu - e$ scattering. Nonvanishing μ_ν will be recognizable only if the corresponding electromagnetic scattering cross section is at least comparable to the well

understood weak interaction cross section. The magnitude of μ_ν (diagonal in flavor or transitional) which can be probed in this way is then given by

$$\frac{|\mu_\nu|}{\mu_B} \equiv \frac{G_F m_e}{\sqrt{2}\pi\alpha}\sqrt{m_e T} \sim 10^{-10}\left(\frac{T}{m_e}\right) , \tag{A.2}$$

where T is the electron recoil kinetic energy. Considering realistic values of T, it would be difficult to reach sensitivities below $\sim 10^{-11}\mu_B$ using the $\nu - e$ scattering. Present limits are about an order of magnitude larger than that.

Limits on μ_ν can also be obtained from bounds on the unobserved energy loss in astrophysical objects. For sufficiently large μ_ν the rate of plasmon decay into the $\nu\bar{\nu}$ pairs would conflict with such bounds. Since plasmons can also decay weakly into the $\nu\bar{\nu}$ pairs , the sensitivity of this probe is again limited by the size of the weak rate, leading to

$$\frac{|\mu_\nu|}{\mu_B} \equiv \frac{G_F m_e}{\sqrt{2}\pi\alpha}\hbar\omega_P , \tag{A.3}$$

where ω_P is the plasmon frequency. Since $(\hbar\omega_P)^2 \ll m_e T$ that limit is stronger than that given in eq.(A.2). Current limits on μ_ν based on such considerations are $\sim 10^{-12}\mu_B$.

The interest in μ_ν and its relation to neutrino mass dates from ∼1990 when it was suggested that the chlorine data[4] on solar neutrinos show an anticorrelation between the neutrino flux and the solar activity characterized by the number of sunspots. A possible explanation was suggested in Ref.[81] where it was proposed that a magnetic moment $\mu_\nu \sim 10^{-(10-11)}\mu_B$ would cause a precession in solar magnetic field of the neutrinos emitted initially as left-handed ν_e into unobservable right-handed ones. Even though later analyses showed that the effect does not exist, the possibility of a relatively large μ_ν accompanied by a small mass m_ν was widely discussed and various models accomplishing that were suggested.

If a magnetic moment is generated by physics beyond the Standard Model (SM) at an energy scale Λ, we can generically express its value as

$$\mu_\nu \sim \frac{eG}{\Lambda}, \tag{A.4}$$

where e is the electric charge and G contains a combination of coupling constants and loop factors. Removing the photon from the diagram gives a contribution to the neutrino mass of order

$$m_\nu \sim G\Lambda. \tag{A.5}$$

We thus have the relationship

$$m_\nu \sim \frac{\Lambda^2}{2m_e}\frac{\mu_\nu}{\mu_B} \sim \frac{\mu_\nu}{10^{-18}\mu_B}[\Lambda(\mathrm{TeV})]^2 \ \mathrm{eV}, \tag{A.6}$$

which implies that it is difficult to simultaneously reconcile a small neutrino mass and a large magnetic moment. These considerations are schematically illustrated in Fig. 27.

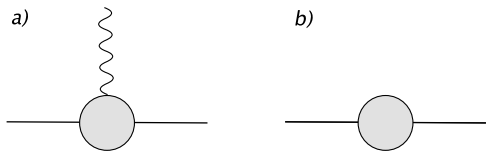

Fig. 27. – a) Generic contribution to the neutrino magnetic moment induced by physics beyond the standard model. b) Corresponding contribution to the neutrino mass. The solid and wavy lines correspond to neutrinos and photons respectively, while the shaded circle denotes physics beyond the SM.

This naïve restriction given in Eq.(A.6) can be overcome via a careful choice for the new physics, e.g., by requiring certain additional symmetries [82, 83, 84, 85]. Note, however, that these symmetries are typically broken by Standard Model interactions. For Dirac neutrinos such symmetry (under which the left-handed neutrino and antineutrino ν and ν^c transform as a doublet) is violated by SM gauge interactions. For Majorana neutrinos analogous symmetries are not broken by SM gauge interactions, but are instead violated by SM Yukawa interactions, provided that the charged lepton masses are generated via the standard mechanism through Yukawa couplings to the SM Higgs boson. This suggests that the relation between μ_ν and m_ν is different for Dirac and Majorana neutrinos. This distinction can be, at least in principle, exploited experimentally, as shown below.

Earlier, I have quoted the Ref.[22] (see Fig.4) to stress that observation of the $0\nu\beta\beta$ decay would necessarily imply the existence of a novanishing neutrino Majorana mass. Analogous considerations can be applied in this case. By calculating neutrino magnetic moment contributions to m_ν generated by SM radiative corrections, one may obtain in this way general, "naturalness" upper limits on the size of neutrino magnetic moments by exploiting the experimental upper limits on the neutrino mass.

In the case of Dirac neutrinos, a magnetic moment term will generically induce a radiative correction to the neutrino mass of order[86]

$$m_\nu \sim \frac{\alpha}{16\pi}\frac{\Lambda^2}{m_e}\frac{\mu_\nu}{\mu_B} \sim \frac{\mu_\nu}{3\times 10^{-15}\mu_B}[\Lambda(\mathrm{TeV})]^2 \ \mathrm{eV}. \tag{A.7}$$

Taking $\Lambda \simeq 1$ TeV and $m_\nu \leq 0.3$ eV, we obtain the limit $\mu_\nu \leq 10^{-15}\mu_B$ (and a more stringent one for larger Λ), which is several orders of magnitude more constraining than current experimental upper limits on μ_ν.

The case of Majorana neutrinos is more subtle, due to the relative flavor symmetries of m_ν and μ_ν respectively. For Majorana neutrinos the transition magnetic moments $[\mu_\nu]_{\alpha\beta}$ are antisymmetric in the flavor indices $\{\alpha,\beta\}$, while the mass terms $[m_\nu]_{\alpha\beta}$ are symmetric. These different flavor symmetries play an important role in the limits, and are the origin of the difference between the magnetic moment constraints for Dirac and Majorana neutrinos.

It has been shown in Ref.[87] that the constraints on Majorana neutrinos are significantly weaker than those for Dirac neutrinos[86], as the different flavor symmetries of m_ν and μ_ν lead to a mass term which is suppressed only by charged lepton masses.

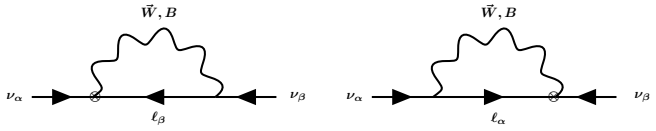

Fig. 28. – One loop diagram contributions to the Majorana neutrino mass associated with the magnetic moment that sum to zero (see [87]). The cross indicates the magnetic moment $[\mu]_{\alpha\beta}$ and the l is the lepton doublet.

This conclusion was reached by considering one-loop mixing of the magnetic moment and mass operators generated by Standard Model interactions. The authors of Ref.[87] found that if a magnetic moment arises through a coupling of the neutrinos to the neutral component of the $SU(2)_L$ gauge boson, the constraints for $\mu_{\tau e}$ and $\mu_{\tau\mu}$ are comparable to present experiment limits, while the constraint on $\mu_{e\mu}$ is significantly weaker. Thus, the analysis of Ref.[87] lead to a model independent bound for the transition magnetic moment of Majorana neutrinos that is less stringent than present experimental limits.

Those considerations are illustrated in Figs. 28, 29.

Even more generally it was shown in Ref.[88] that two-loop matching of mass and magnetic moment operators implies stronger constraints than those obtained in[87] if the scale of the new physics $\Lambda \geq 10$ TeV. Moreover, these constraints apply to a magnetic moment generated by either the hypercharge or $SU(2)_L$ gauge boson. In arriving at these conclusions, the most general set of operators that contribute at lowest order to the mass and magnetic moments of Majorana neutrinos was constructed, and model independent constraints which link the two were obtained. Thus the results of Ref.[88] imply completely model independent naturalness bound that – for $\Lambda \geq 100$ TeV – is stronger than present experimental limits (even for the weakest constrained element $\mu_{e\mu}$). On the other hand, for sufficiently low values of the scale Λ the known small values of the neutrino masses do not constrain the magnitude of the magnetic moment μ_ν more than the present experimental limit. Thus, if these conditions are fulfilled, the discovery of μ_ν might be forthcoming any day.

The above result means that an experimental discovery of a magnetic moment near the present limits would signify that (i) neutrinos are Majorana fermions and (ii) new

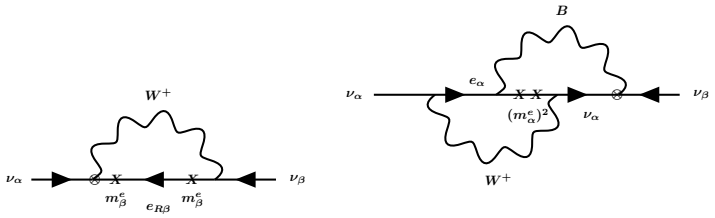

Fig. 29. – The one and two loop contributions to the Majorana neutrino mass associated with the magnetic moment. Here X is the charged lepton mass insertion (see [87]).

lepton number violating physics responsible for the generation of μ_ν arises at a scale Λ which is well below the see-saw scale. This would have, among other things, implications for the mechanism of the neutrinoless double beta decay and lepton flavor violation as discussed above and in Ref.[28].

* * *

The original results reported here were obtained in collaboration with Nicole Bell, Vincenzo Cirigliano, Jonathan Engel, Amand Faessler, Michail Gorchtein, Andryi Kurylov, Gary Prezeau, Michael Ramsey-Musolf, Vadim Rodin, Fedor Šimkovic, Peng Wang and Mark Wise. The fruitful collaboration with them is gratefully acknowledged.

REFERENCES

[1] Kajita T and Totsuka Y, *Rev. Mod. Phys.* 73, 85-118 (2001); Y. Ashie et al., *Phys. Rev.* D71, 112005 (2005).
[2] Ahn MH *et al.*, *Phys. Lett. B* 511, 178-184 (2001); Ahn MH *et al.* hep-ex/0606032.
[3] MINOS collaboration, hep-ex/0607088; arXiv:0708.1495.
[4] Cleveland BT *et al.*, *Astrophys. J.* 496, 505 (1998).
[5] Ahmad QR *et al.*, *Phys. Rev. Lett.* 87, 071301 (2001).
[6] Fukuda S *et al.*, *Phys. Rev. Lett.* 86, 5651-5655, (2001); ibid 86, 5656-5660 (2001).
[7] Hampel W *et al. Phys. Lett.* B447, 127 (1999).
[8] Abdurashitov JN *et al. Phys. Rev.* C60, 055801 (1999).
[9] Eguchi K *et al. Phys. Rev. Lett.* 90, 021802 (2003).
[10] Araki T *et al. Phys. Rev. Lett.* 94, 081801 (2005).
[11] Abe S *et al.*, arXiv:0801.4589.
[12] Apollonio M *et al.*, *Phys. Lett. B* 466, 415-430 (1999).
[13] Boehm F *et al.*, *Phys. Rev.* D64, 112001 (2001).
[14] Weinberg S, *Phys. Rev. Lett.* 43, 1566 (1979).
[15] Gell-Mann M, Ramond P, and Slansky R, in *Supergravity*, eds. D. Freeman and P. Niuwenhuizen, North Holland, 1979; Yanagida T, in *Proceedings of Workshop on Unified Theory and Baryon Number of Universe*, eds. O. Sawada and A. Sugamoto, KEK, Tsukuba, 1979; Mohapatra R and Senjanovic G, *Phys. Rev. Lett* **44**, 912 (1980); Minkowski P, *Phys. Lett. B* **67**, 421 (1977).
[16] Faessler A and Šimkovic F, *J. Phys. G* 24, 2139 (1998).
[17] Suhonen J and Civitarese), *Phys.Rep.***300**, 123(1998).
[18] Vergados JD, *Phys. Rep.* 361, 1 (2002).
[19] Elliott SR and Vogel P *Ann.Rev.Nucl.Part.Sci.* 52, 115 (2002).
[20] Elliott SR and Engel J, *J. Phys. G* 30, R183 (2004).
[21] Avignone FT, Elliott SR and Engel J, *Rev. Mod. Phys.*, **80**, 481 (2008); arXiv:0708.1033.
[22] Schechter J and Valle J, *Phys.Rev.* D25, 2951 (1982).
[23] Boehm F and Vogel P, *Physics of Massive Neutrinos*, 2nd ed., Cambridge Univ. Press, Cambridge, 1992.

[24] Mohapatra RN, *Phys. Rev. D***34**, 3457(1986); Vergados JD, *Phys. Lett. B* **184**, 55(1987); Hirsch M, Klapdor-Kleingrothaus HV, and Kovalenko SG, *Phys. Rev. D***53**, 1329(1996); Hirsch M, Klapdor-Kleingrothaus HV, and Panella O, *Phys. Lett. B* **374**, 7(1996); Fässler A, Kovalenko S, Šimkovic F, and Schwieger J, *Phys. Rev. Lett.* **78**, 183(1997); Päs H, Hirsch M, Klapdor-Kleingrothaus HV, and Kovalenko SG, *Phys. Lett. B* **498**, 35(2001); Šimkovic F and Fässler A, *Progr. Part. Nucl. Phys.* **48**, 201(2002).
[25] Prezeau G, Ramsey-Musolf MJ and Vogel P, *Phys. Rev. D* **68**, 034016 (2003).
[26] Mohapatra RN, *Nucl. Phys. Proc. Suppl.* **77**, 376 (1999).
[27] Doi M, Kotani T, and Takasugi E, *Prog. Theor. Phys. Suppl.* **83**, 1(1985).
[28] Cirigliano V, Kurylov A, Ramsey-Musolf MJ and Vogel P, *Phys.Rev.Lett* **93**, 231802 (2004).
[29] Signorelli G, *"The Meg Experiment At Psi: Status And Prospects," J. Phys. G* **29**, 2027 (2003); see also http://meg.web.psi.ch/docs/index.html.
[30] Popp JL, *NIM* **A472**, 354 (2000); hep-ex/0101017.
[31] Brooks ML *et al. Phys.Rev.Lett.***83**, 1521 (1999).
[32] Bertl W *et al.* PSI report, unpublished; (2002)
[33] Barbieri R, Hall LJ and Strumia A, *Nucl. Phys. B* **445**, 219 (1995)
[34] Arganda E, Herrero MJ, and Teixeira AM, arXiv:0707.2955.
[35] Albright CH and Chen M-C, arXiv:0802. 4228 [hep-ph].
[36] Borzumati F and Masiero A *Phys.Rev.Lett.***57**, 961 (1986).
[37] Barbieri R andHall LJ, *Phys. Lett. B* **338**, 212 (1994).
[38] Raidal M and Santamaria A, *Phys. Lett. B* **421**, 250 (1998).
[39] Kitano R, Koike M and OkadaY, *Phys. Rev. D* **66**, 096002 (2002).
[40] Dreiner H., in *"Perspectives on Supersymmetry"*, Ed. by G.L. Kane, World Scientific, 462-479.
[41] de Gouvea A, Lola S and Tobe K, *Phys. Rev. D* **63**, 035004 (2001).
[42] Mohapatra RN and Senjanovic G, *Phys. Rev. Lett.* **44**, 912 (1980).
[43] Cirigliano V, Kurylov A, Ramsey-Musolf MJ and Vogel P, *Phys. Rev. D* **70**, 075007 (2004).
[44] Elliott SR, Hahn AA and Moe MK, *Phys. Rev. Lett.* **59**, 2020 (1987).
[45] Klapdor-Kleingrothaus H.V. *et al. Eur.J.Phys.* A12, 147 (2001).
[46] Aalseth C. E. *et al. Phys.Rev.* D65, 092007 (2002).
[47] Arnaboldi C *et al.*, arXiv:0802.3439.
[48] Klapdor-Kleingrothaus HV , Dietz A, Krivosheina IV, and Chvorets O *Phys. Lett.* B586, 198 (2004); *Nucl. Inst. Meth* A522, 371 (2004); Klapdor-Kleingrothaus HV and Krivosheina IV, *Mod. Phys. Lett. A***21**, 1547(2006).
[49] Wycech S and Sujkowski Z, *Phys. Rev. C***70**, 052501(2004).
[50] Bernabeu J, DeRujula A, and Jarlskog C, *Nucl. Phys. B***223**, 15 (1983).
[51] Flack RL in *Neutrino98*, www2.phys.cantebury.ac.nz/ jaa53/presentations/flack.pdf.
[52] Primakoff H and Rosen SP, *Rep.Prog. Phys.***22**, 121 (1959).
[53] Doi M *et al. Progr. of Theor. Phys. Suppl.* **83** (1985).
[54] Ericson T and Weise W, *Pions and Nuclei* (Clarendon, Oxford, 1988), pp. 423-426.
[55] Rodin VA, Faessler A, Šimkovic F and Vogel P, Nucl. Phys.**A766**, 107 (2006) and erratum, Nucl. Phys. **A793**,213(2007); arXiv:0706.4304.
[56] Nowacki F, talk at the IDEA meeting, Heidelberg, Oct. 2004.
[57] Retamosa J, Caurier E and Nowacki F, *Phys. Rev. C***51**, 371(1995).
[58] Caurier E, Nowacki F, Poves A, and Retamosa J, *Phys. Rev. Lett.* **77**, 1954 (1996).
[59] Caurier E, Nowacki F, Poves A, and Retamosa J, *Nucl. Phys. A***654**, 973c (1999).
[60] Caurier E, Martinez-Pinedo G, Nowacki F, Poves A, and Zuker A, *Rev. Mod. Phys.***77**, 427 (2005).
[61] Caurier E, Menendez J, Nowacki F, and Poves A, *Phys. Rev. Lett.* **100**, 052503 (2008); arXiv:0708.2137.

[62] Caurier E, Nowacki F and Poves A, arXiv:0708.0277.
[63] Menendez J, Poves A, Caurier E, and Nowacki F, arXiv:0801.3760.
[64] Halbleib JA and Sorensen RA, *Nucl. Phys.*bf A98, 542 (1967).
[65] Cha D, *Phys. Rev. C***27**, 2269(1983).
[66] Šimkovic F, Faessler A, Rodin VA, and Vogel P, *Phys. Rev.* C77, 045503 (2008).
[67] Toivanen J and Suhonen J, *Phys. Rev. Lett.* 75, 410 (1995).
[68] Faessler A and Šimkovic F, *J. Phys. G***24**, 2139 (1998).
[69] Vogel P and Zirnbauer MR, *Phys. Rev. Lett.* 57, 3148 (1986).
[70] Suhonen J, *Phys. Lett.* **B607**, 87 (2005)
[71] Griffiths A and Vogel P, *Phys. Rev.C* **46**, 181 (1992).
[72] Rodin VA, Faessler A, Šimkovic F and Vogel P, *Nucl. Phys.***A766**, 107 (2006) and erratum, *Nucl. Phys.* **A793**,213(2007); arXiv:0706.4304.
[73] Rodin VA, Faessler A, Šimkovic F and Vogel P, it Phys. Rev. C **68**, 044302 (2003).
[74] Bahcall JN, Murayama H, and Pena-Garay C, *Phys. Rev. D* **70**, 033012 (2004).
[75] G. A. Miller and J. E. Spencer, *Ann. Phys.* **100**, 562 (1976).
[76] A. Fabrocini, F. A. de Saavedra and G. Co', *Phys. Rev. C* **61**, 044302 (2000), and G. Co', private communication.
[77] H. Feldmeier, T. Neff, R. Roth and J. Schnack, *Nucl. Phys.* **A632**, 61 (1998).
[78] Kortelainen M and Suhonen J, *Phys. Rev. C* **75**, 051303 (2007); ibid *Phys. Rev. C* **76**, 024315 (2007); Kortelainen M, Civitarese O, Suhonen J, and Toivanen J, *Phys. Lett.* **B647**, 128 (2007).
[79] Šimkovic F, Pantis G, Vergados JD, and Fässler A, *Phys. Rev. C* **60**, 055502 (1999),
[80] Marciano WJ and Sanda AI, *Phys. Lett.* **B67**, 303 (1977); Lee BW and Shrock RE *Phys. Rev.D* **16**, 1444 (1977); Fujikawa K and Shrock RE *Phys. Rev. Lett.* **45**, 963 (1980).
[81] Voloshin MB, Vysotskij MI and and Okun LB, *Soviet J. of Nucl. Phys.* **44**, 440 (1986).
[82] Voloshin MB, *Sov. J. Nucl. Phys.***48**, 512 (1988). For a specific implementation see Barbieri R and Mohapatra RN, *Phys. Lett.* **B218**, 225(1989).
[83] Georgi H and Randall L, *Phys. Lett.* **B244**, 196(1990).
[84] Grimus W and Neufeld H, *Nucl. Phys. B***351**, 115 (1991).
[85] Babu KS and Mohapatra RN, *Phys. Rev. Lett.* **64**, 1705 (1990).
[86] Bell NF *et al.*, *Phys. R. Lett.* **95**, 151802 (2005).
[87] Davidson S, Gorbahn . and Santamaria A, *Phys. Lett.* **B626**, 151 (2005).
[88] Bell NF*et al.*, Phys. Lett. **B642**, 377 (2006); hep-ph/0606248.